N84-22524

aer

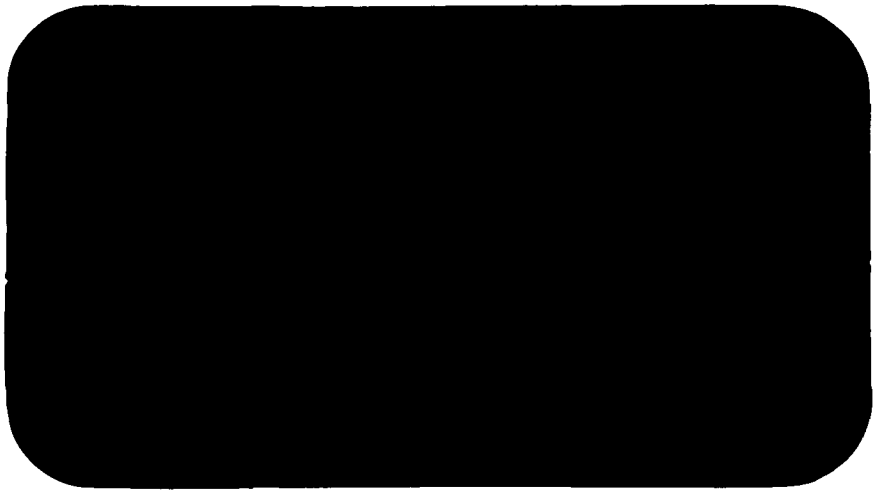

ATMOSPHERIC AND ENVIRONMENTAL RESEARCH, INC.
CAMBRIDGE, MASSACHUSETTS

OUTER SATELLITE ATMOSPHERES: THEIR EXTENDED NATURE AND PLANETARY INTERACTIONS

William H. Smyth
and
Michael R. Combi

Atmospheric and Environmental Research, Inc.
840 Memorial Drive
Cambridge, Massachusetts 02139

April 1984

Interim Report for Period
December 1, 1983 to February 29, 1984

Prepared for
NASA Headquarters

TECHNICAL REPORT STANDARD TITLE PAGE

1 Report No	2 Government Accession No	3. Recipient's Catalog No.

4 Title and Subtitle	5. Report Date
Outer Satellite Atmospheres: Their Extended Nature and Planetary Interactions	April 1984
	6 Performing Organization Code
7 Author(s)	8 Performing Organization Report No
William H. Smyth and Michael R. Combi	
9 Performing Organization Name and Address	10 Work Unit No
Atmospheric and Environmental Research, Inc. 840 Memorial Drive Cambridge, Massachusetts 02139	11 Contract or Grant No. NASW-3387
	13 Type of Report and Period Covered Interim Report December 1983 - February 1984
12 Sponsoring Agency Name and Address	14 Sponsoring Agency Code
NASA Headquarters Headquarters Contract Division Washington, DC 20546	HW-2
15. Supplementary Notes	

16 Abstract

Model calculations for the brightness of the sodium cloud in Region A were performed to clarify the role played by the plasma torus sink in producing the east-west intensity asymmetry observed in the sodium D-lines. It was determined that the east-west electric field, proposed by Barbosa and Kivelson (1983) and Ip and Goertz (1983) to explain the dawn-dusk asymmetry in the torus ion emissions measured by the Voyager UVS instrument, could also produce the east-west sodium intensity asymmetry discovered earlier by Bergstralh et al. (1975, 1977). Model results for the directional features of the sodium cloud were also reported. The completion of the development of the Io potassium cloud model, progress in improving the Titan hydrogen torus model, and efforts in developing our model for hydrogen cometary atmospheres were also discussed.

17 Key Words (Selected by Author(s))	18 Distribution Statement
satellite atmospheres planetary magnetospheres comets	

19 Security Classif. (of this report)	20 Security Classif. (of this page)	21. No of Pages	22 Price*
Unclassified	Unclassified		

*For sale by the Clearinghouse for Federal Scientific and Technical Information, Springfield, Virginia 22151

I. SUMMARY OF RESEARCH PERFORMED IN THE THIRD QUARTER

Research activities in the past quarter have been focused upon (1) further modeling studies of the Io sodium cloud for region A and Region C, (2) development and preliminary testing of our Io potassium cloud model, (3) continued evaluation of magnetospheric plasma data for Saturn to be used in our Titan hydrogen torus model, and (4) collection and initial evaluation of Lyman α profile data for use in our comet particle trajectory model.

1. Spatial Morphology of the Sodium Cloud

Region A

The east-west intensity asymmetry of Region A, discovered and documented by Bergstralh et al. (1975 and 1977), was recently attributed by Smyth (1983) to the effects of both solar radiation pressure (for very low velocity escape of sodium from Io) and the plasma torus sink (for higher velocity escape of sodium from Io). The need, noted by Smyth (1983), to further clarify the role played by the Io plasma torus sink, has been initially addressed this past quarter. This has been accomplished by using our new Io sodium cloud model, which explicitly includes the oscillating plasma torus sink, to calculate the brightness of Region A as viewed through the rectangular viewing slit adopted by Bergstralh et al. (1975, 1977). The effects of the oscillating plasma torus sink, the presence of an east-west electric field in the magnetosphere (Ip and Goertz, 1983; Barbosa and Kivelson, 1983), and the impact of the offset dipole nature of the planetary magnetic field (Acuña, Behannon, and Connerney, 1983) have been preliminarily assessed and are briefly discussed here. More quantitative results will be presented in the final report.

The oscillation of the plasma torus about the satellite plane introduces a modulation in the brightness of Region A because of the varying sodium lifetime at Io, but it does not introduce any east-west intensity asymmetry (if the plasma properties are independent of system III magnetic longitude). An east-west electric field in the magnetosphere has recently been proposed by Ip and Goertz (1983) and Barbosa and Kivelson (1983) to explain the dawn-dusk asymmetry in the torus ion emission brightness measured by the Voyager UVS instrument (Sandel and Broadfoot, 1982; Shemansky and Sandel, 1982). The electric field essentially shifts the plasma torus to a new center that is

displaced toward the east by about 0.18 to 0.20 Jupiter radii. For a given radial displacement from Jupiter, this provides an overall east to west shift of the plasma torus properties by twice this amount and gives rise to a significant east-west asymmetry in the sodium sink because of the sharp temperature gradient inside of Io's orbit. This asymmetry in the sink provides an east-west intensity asymmetry in the brightness of Region A that is in agreement with the value observed by Bergstralh et al. (1975, 1977). Inclusion of the offset dipole magnetic field in the sodium model provides a modulation of the east-west intensity asymmetry about the mean value established by the east-west electric field. This modulation may account for some of the apparent scatter present in the intensity data of Bergstralh et al. (1975, 1977).

Region C

The directional features of the sodium cloud, discovered by Pilcher (see Hartline, 1980), extend from Region B into Region C. Within the past year, changes in the north-south directions of these features have been successfully understood through our model-data comparisons which have involved an active collaborative effort with Pilcher. The extremely interesting results of this collaborative effort are presented in a paper submitted in the past quarter to The Astrophysical Journal for publication. A copy of this paper is attached as an appendix to this progress report. Our paper is to be published jointly with a companion paper entitled "Ejection of Atoms and Molecules from Io by Plasma-ion Impact" submitted by E.M. Sieveka and R.E. Johnson of the University of Virginia.

In short, the directional features can result from a source of high velocity ($\sim$20 km sec^{-1}) sodium combined with the oscillating neutral sodium sink provided by the plasma torus. The phase relationship between the features' directions and Io's magnetic longitude can be understood if escaping sodium is initially directed at near right angles to Io's orbital motion. The initial directions and speeds of sodium atoms escaping Io to form the directional features can be understood in terms of a magnetospheric-wind-driven escape mechanism. The companion paper submitted by E.M. Sieveka and R.E. Johhnson addresses the subject of ejection of sodium atoms from Io and provides support for the magnetospheric-wind-driven escape mechanism.

2. Io Potassium Cloud Model

The development of a model for the Io potassium cloud has been completed this past quarter. The model contains all the refinements present in our most recent Io sodium cloud model. The lifetime of potassium, determined for electron impact ionization, may be specified for plasma conditions reflecting the encounter times of Voyager 1 and Voyager 2 with Jupiter. In calculating the brightness of the cloud as well as the acceleration effects of solar radiation pressure, the solar spectra for the 7665 Å and 7699 Å lines of potassium as determined for our model by Kurucz (1982) and reported in our last annual report (i.e., June 1, 1981 to May 31, 1982 period) were adopted in the model. The model has undergone initial testing and preliminary model runs are anticipated in the next quarter.

3. Titan Hydrogen Torus Modeling

Effort this quarter has been limited to examining the two-dimensional (radial and vertical) density and temperature information for ions and electrons in Sturn's magnetosphere supplied recently by Sittler (1983). This information will be incorporated in the Titan torus model in the last quarter to calculate the lifetime of hydrogen in the circumplanetary environment.

4. Modeling of Cometary Hydrogen

The full solar disk Lyman-α profile as determined by Lemaire et al. (1978) has been adopted for use in our comet particle-trajectory model. This profile, shown in Figure 1, is the only available high-resolution full disk Lyman-α profile of the Sun (Skumanich, 1984). The profile has been put in digital form for use by the model. In our model calculations for the extended hydrogen cloud, the profile will be utilized to calculate the radiation pressure acceleration of H atoms and their brightness produced by solar resonance scattering. The process of incoporating the profile into the model, initiated in the past three months, will be completed during the next quarter.

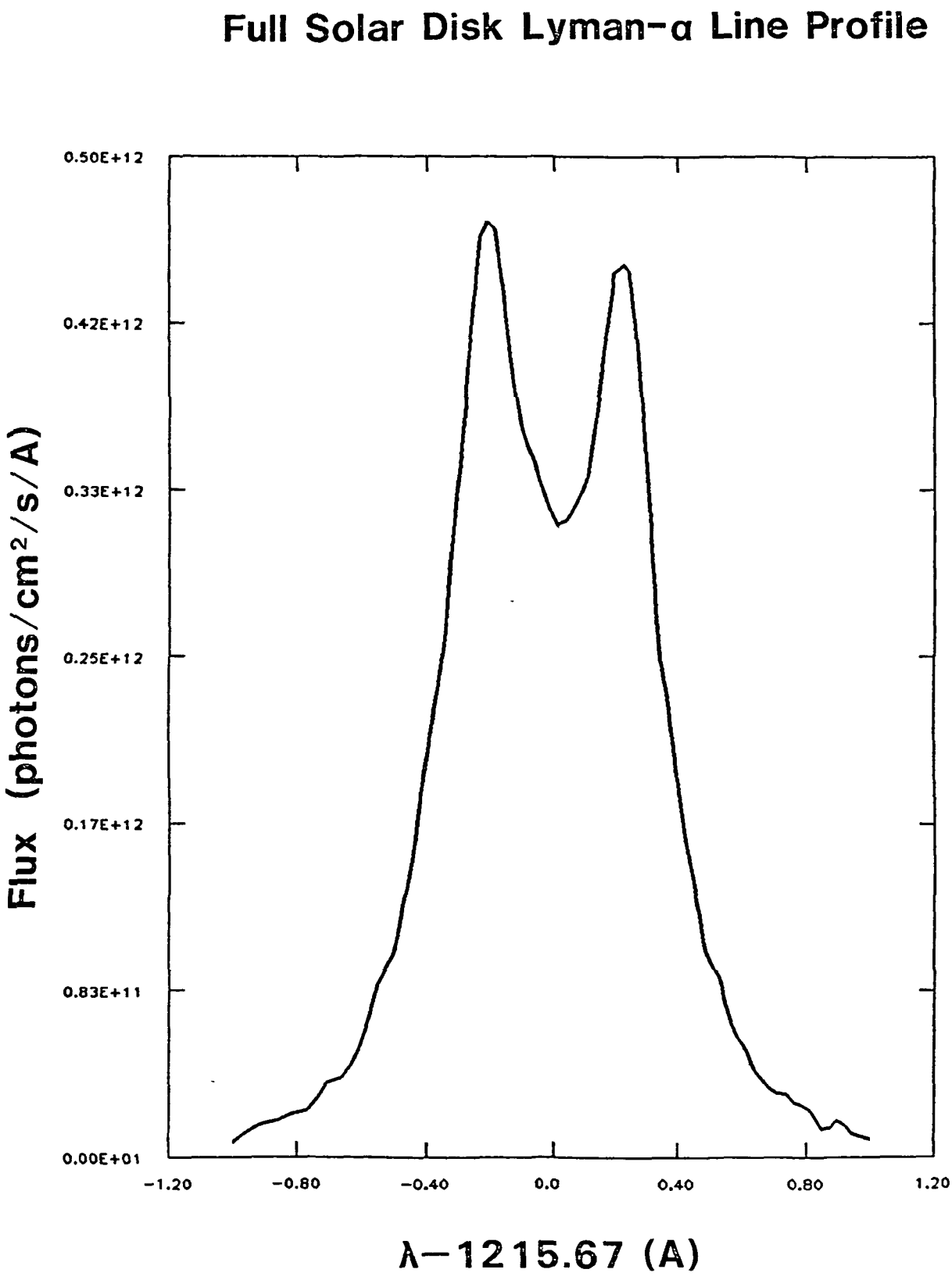

Figure 1. Full Solar Disk Lyman-α Line Profile. The profile was determined by Lemaire et al (1978).

II. Program for the Last Quarter

Research activities in the last quarter will involve (1) implementing the Saturn magnetospheric plasma data in our Titan torus model and performing preliminary model calculations, (2) completing the incorporation of the Lyman-α profile in the comet particle trajectory model and performing initial model calculations for the extended H atmospheres of comets, and (3) performing preliminary model calculations for the Io potassium cloud.

REFERENCES

Acuña, M.H., K.W. Behannon and J.E.P. Connerney (1983) Jupiter's Magnetic Field and Magnetosphere. In Physics of the Jovian Magnetosphere, (ed. A.J. Dessler), Cambridge University Press, pp. 1-50.

Barbosa, D.D. and M.G. Kivelson (1983) Dawn-Dusk Electric Field Asymmetry of the Io Plasma Torus. Geophys. Res. Lett. 10, 210.

Bergstralh, J.T., D.L. Matson and T.V. Johnson (1975) Sodium D-line Emission from Io: Synoptic Observations from Table Mountain Observatory. Ap. J. Lett. 195, L131.

Bergstralh, J.T., J.W. Young, D.L. Matson and T.V. Johnson (1977) Sodium D-Line Emission from Io: A Second Year of Synoptic Observation from Table Mountain Observatory. Ap. J. Lett. 211, L51.

Hartline, B.K. (1980) Voyager Beguiled by Jovian Carrousel. Science 208, 384.

Ip, W.-H. and C.K. Goertz (1983) An Interpretation of the Dawn-Dusk Asymmetry of UV Emission from the Io Plasma Torus. Nature 302, 232.

Kurucz, R.L. (1983) Private communication.

Lemaire, P., J. Charra, A. Jouchoux, A. Vidal-Madjar, G.E. Artzner, J.C. Vial, R.M. Bonnet and A. Skumanich (1978) Calibrated Full Disk Solar H I Lyman-α and Lyman-β Profiles. Ap. J. 223, L55.

Sandel, B.R. and A.L. Broadfoot (1982) Io's Hot Plasma Torus - A Synoptic View from Voyager. J. Geophys. Res. 87, 212.

Shemansky, D.E. and B.R. Sandel (1982) The Injection of Energy into the Io Plasma Torus. J. Geophys. Res. 87, 219.

Sittler, E.C. (1983) Private communication.

Skumanich, A. (1984) Private communication.

Smyth, W.H. (1983) Io's Sodium Cloud: Explanation of the East-West Asymmetries. II. Ap. J. 264, 708.

IO'S SODIUM DIRECTIONAL FEATURES: EVIDENCE FOR A MAGNETOSPHERIC-WIND-DRIVEN GAS ESCAPE MECHANISM

by

C. B. Pilcher*
W. H. Smyth†
M. R. Combi†
J. H. Fertel*

*Institute for Astronomy, University of Hawaii, Honolulu, Hawaii

†Atmospheric and Environmental Research, Inc., Cambridge, Massachussetts

ABSTRACT

Elongated features in Io's sodium cloud, directed away from Jupiter and both to the north and south of the satellite's orbital plane, have been observed. The north/south directions of the features are correlated with Io's magnetic longitude, suggesting a formation mechamism involving the oscillating plasma torus. We show by means of a model analysis that the features can result from a source of high velocity ($\sim$ 20 km sec^{-1}) sodium combined with the oscillating neutral sodium sink provided by the plasma. The phase relationship between the features' directions and Io's magnetic longitude can be understood if escaping sodium is initially directed at near right angles to Io's orbital motion. The directionality of the features requires that the sodium flux from equatorial regions be higher than that from the poles. The initial directions and speeds of sodium atoms escaping Io to form the directional features can be understood in terms of a magnetospheric-wind-driven escape mechanism. The one sequence of directional feature observations that we have analyzed in detail implies a high speed sodium source rate of $\sim 10^{26}$ atoms sec^{-1}.

I. INTRODUCTION

Sodium D-line emission in the spectrum of Io, Jupiter's innermost Galilean satellite, was discovered by Brown (1974; Brown and Chaffee, 1974). Shortly thereafter, it was determined that this emission emanates from a substantial volume of space surrounding the satellite (Trafton et al. 1974; Mekler and Eviatar, 1974; Wehinger and Wyckoff, 1974). The morphology of the sodium cloud, discussed in the review by Pilcher and Strobel (1982), leaves no doubt that the sodium originates on Io. The directions and velocity dispersion of the atoms ejected from Io to populate the cloud have been a topic of considerable study, involving the analysis of both sodium D-line profile data and spatial intensity data. No escape mechanism has yet been identified, however, that can properly explain both these spectral and spatial signatures.

Trafton (1975) and Trafton and Macy (1977) have shown that the center of the sodium D-line, measured with Io in the field of view, exhibits a wavelength shift which depends upon the orbital phase of the satellite. In addition, the line profile shows an asymmetric wing (or skirt) extending to doppler shifts relative to Io of up to 18 km sec^{-1}. The skirt appears to be stronger when Io is near the magnetic equator. The asymmetric skirt is seen on the blue side of the line center when Io is near eastern elongation and on the red side when Io is near western elongation, so that the sodium atoms producing it always appear to be traveling more rapidly in the direction of Io's motion than the satellite. In analyzing these observations, Trafton and Macy (1978) concluded that the asymmetric skirt was produced by high-speed sodium ($\leq$20 km sec^{-1}) streaming from Io, preferentially in the direction of the satellite's orbital motion, and that the line core could be produced either by an atmosphere stationary with respect to Io or by a cloud expanding primarily at low velocities ($\leq$3 km sec^{-1}). They showed that a speed dispersion composed of a primary low-velocity peak for the line center and a secondary (but broader) high-velocity peak for the asymmetric skirt was sufficient to reproduce the characteristics of their data.

Smyth and McElroy (1977) presented line profile calculations for Io at eastern elongation to explain the general characteristics observed in the data of Trafton (1975). They concluded that sodium ejected primarily from the leading inner quadrant of the satellite at velocities near 3 km sec^{-1} would explain

the shift of the line center and that a speed dispersion ranging up to 15 km sec^{-1} would produce the asymmetric skirt. Carlson et al. (1978) analyzed three profiles: one line profile which they measured 8 arc seconds from Io with the satellite almost 45 degrees past western elongation, and two different line profiles measured by Trafton (1975), one of which was independently analyzed by Trafton and Macy (1978). Carlson et al. concluded that these three observations were best matched by sodium atoms ejected from Io's leading hemisphere with a velocity dispersion that must be similar to the sputtering distribution that they adopted. The velocity distribution they assumed peaks at ~3 km sec^{-1} and extends to velocities as high as those inferred by Trafton and Macy (1977). Using the model of Carlson et al. (1978), Porco, Trauger and Carlson (Trauger, 1980) also analyzed a line profile that they measured near the satellite when Io was at western elongation. They found that their observation was explained by radial sodium ejection from the satellite hemisphere centered on the sub-Jupiter point (i.e., the inner hemisphere).

Although the exact angular and velocity dispersions of sodium are not very well defined by the rather broad hemispherical source regions adopted in the above analyses, certain primary conclusions emerge. To explain the line profile shapes, sodium ejected from Io must be described by a velocity distribution that includes speeds up to 20 km sec^{-1}; many of these high-speed atoms must have a significant velocity component in the direction of Io's motion. Since the preferential direction of these velocity components is in the same direction as that of the magnetospheric plasma moving past Io, and since the size of the asymmetric line profile wing appears to be correlated with Io's magnetic latitude, a dependence of the sodium source on the magnetospheric flow is suggested. Furthermore, from the direction and magnitude of the high-speed sodium, one would also expect to observe sodium at a considerable distance from Io. Sodium emission has in fact been reported in Jupiter's equatorial plane at distances as large as ~35 R_J (Pilcher and Schempp, 1979) and ~53 R_J (Trafton and Macy, 1978) from the planet. These distances should be compared to Io's orbital radius of ~6 R_J.

More recent D-line profile data have been obtained by Brown and Schneider (1981) at distances up to 20 R_J from Jupiter. In most spectra they observed a narrow emission feature which they concluded was due to sodium atoms on bound orbits with apojoves in the field of view and perijoves near Io's orbit. Ejec-

tion from Io in the forward direction at velocities relative to the satellite of 2-4 km/sec would yield atoms on the inferred orbits. On two occasions, however, Brown and Schneider observed a broad emission feature whose central wavelength corresponded to a velocity of ~30 km/sec relative to Jupiter and which exhibited a tail extending to atomic velocities of ≤100 km/sec in Jupiter's rest frame. They attributed this feature to some combination of charge exchange between neutral and corotating ionized sodium, and elastic collisions between sodium atoms and corotating heavy ions. They noted that the rates of both of these processes should be at a maximum when Io is near the symmetry plane of the plasma torus, and that their two observations projected back in time to this geometry. Brown and Schneider noted that although the velocities they measured were considerably higher than those reported by Trafton and Macy, their observations and those of the latter authors were likely related.

Spatial intensity measurements of the sodium region-B cloud in Io's immediate vicinity appear to provide information primarily on material that left Io at relatively low velocities. Matson et al. (1978) presented two images showing a banana-shaped cloud surrounding Io with more sodium atoms preceding the satellite in its orbit than following. They found they could account for this shape by assuming sodium atoms were ejected with a velocity distribution characteristic of ion sputtering from a hemisphere intermediate between Io's leading hemisphere and that facing Jupiter. Smyth and McElroy (1978), analyzing a set of 56 images of the region-B cloud obtained by Murcray and Goody (1978; also see Murcray, 1978), concluded that sodium appears to originate on the inner hemisphere or some combination of the inner and trailing hemispheres of Io. They found that the data could be matched by models with a relatively constant hemispheric source of 2×10^{25} atoms sec^{-1}, ejected at a characteristic velocity of 2.6 km sec^{-1} relative to Io. Their results indicate that the data of Matson et al. (1978) can probably be accounted for by the low velocity peak in the sputtering velocity distribution. An improved Io sodium cloud model including the effects of the oscillating plasma torus, used in this paper to analyze the newly discovered sodium directional features, has recently been applied to the region-B cloud (Smyth and Combi, 1983). Because of the inclusion of this severe, spatially non-uniform sink for sodium, it now appears that the observations of Murcray and Goody (1978) can be explained by low-velocity sodium ejected symmetrically from Io's inner and outer hemispheres with an increased source rate of about 2×10^{26} sec^{-1}.

In this paper we report the results of an imaging study of the sodium D_2-line intensity in the vicinity of Io which shows the effects of high velocity ejection from the satellite. The manifestation in our data is in the form of previously unrecognized directional features. We show that the features, which are directed away from Jupiter and appear to oscillate north and south of Io's orbital plane, may be explained in terms of a high velocity sodium source and an oscillating sink provided by the Io plasma torus. The directions and velocities of sodium atoms required to account for these features provide direct evidence for a magnetospheric-wind-driven gas escape mechanism from Io. We also show that during a portion of February 1980, the sodium emission intensity surrounding Io, including that of the directional features was anomalously high. The difference with prior and subsequent observations indicates that this was a period of unusual activity on or near the satellite.

II. OBSERVATIONAL AND DATA REDUCTION TECHNIQUES

We obtained sodium D_2-line images using a 2.5-Å bandwidth (FWHM) interference filter and an image-tube/photographic-plate detector on the 2.2-m telescope at Mauna Kea Observatory in the manner described by Pilcher (1980). A 14-arcsecond diameter occulting disk in the form of 1.5-mm aluminum dot deposited on a window in the telescope focal plane was used to prevent light from Io's disk from entering the optical system. The field of view was 110 arcseconds in diameter, which corresponded to 5.0 to 5.5 R_J depending upon the geocentric distance of Jupiter at the time of the observation. Exposure times were generally three minutes. The interference filter was designed so that at 0°C and normal incidence its passband was centered slightly (~4 Å) to the red of the rest wavelength of the sodium D_2 line (5890.0 Å). We tilted the filter to tune it toward the blue for the observations.

It is possible to do these observations with or without a collimator preceding the filter in the optical train. If a collimator is not used, then the divergence angle of the beam emanating from any image point in the telescope focal plane will cause different portions of the beam to be transmitted by the filter at somewhat different wavelengths. In this application the result would be a loss in contrast between the monochromatic image and the background continuum. Since we wished to detect the faintest radiation possible, we chose to collimate the beam from the telescope. This, however, introduced another variation. Collimated bundles from different points in the telescope focal plane do not strike the filter at the same angle. For a monchromatic source, the effect is a variation in the transmission across the field of view. This is illustrated in Figure 1, in which we show a sequence of three-minute exposures taken at filter tilts separated by 1°. These images were taken when Io was within a few degrees of western elongation. In Figure 2 we show contour plots of the system spatial transmission corresponding to three of these images. The spatial transmission functions were derived from room temperature, laboratory tracings of the filter transmission and an empirical correction for the change in central wavelength with temperature determined from a comparison of the laboratory and Jovian data. It is clear from Figures 1 and 2 that although the transmission in this case at filter tilt angles of 1° or 2° is sufficiently uniform to show sodium emission over the entire field, this is not so at higher tilt angles. Since approximate spatial transmission functions are known, it is

possible to correct images for this effect in all areas where sodium emission has been detected and the system transmission function is significantly above zero. All of the contour plots presented below have been corrected in this manner.

The data were traced on a Perkin-Elmer PDS 1010A microdensitometer controlled by means of a DEC PDP 11/40 minicomputer. The digitization interval was ~0.5 arcseconds and the scanning aperture width was slightly less than the spacing between samples. For later processing and display in the form of contour maps, 4 x 4 pixels of each image were averaged. This filtering yielded higher signal-to-noise ratio, but a resolution of only ~2 arcseconds or ~0.1 R_J. Since the seeing and telescope tracking were generally better than this value, this is the approximate spatial resolution of the digital data in final form.

Before filtering or background subtraction (see below) we converted approximately from photographic density to relative intensity using calibration curves obtained during spectroscopic observations on other nights. Calibration curves obtained on several nights did not vary significantly from one another at relative intensities below 400 (arbitrary units). At higher relative intensities, however, the curves sometimes diverged, and in no cases did the curves extend beyond 600. Our relative intensity scale (uncorrected for system spatial transmission) should therefore be regarded as only an estimate at values much above 400. This statement applies particularly to data obtained during February 1980 in which values exceeding 1000-2000 are common. For images such as these, in which the maximum photographic density exceeds the maximum density on the calibration plates, we extrapolated the calibration curves. The inaccuracies inherent in this procedure render these high relative intensity values useful only as indicators of extremely bright emission.

In general, we obtained images in sequences of increasing filter tilt angle. The angular increment was 1° and the sequences usually extended to angles (~6°) at which essentially no D-line radiation was transmitted. The best such image for each night was used as a measure of the background and subtracted from each D-line image obtained on that night. All of the contour plots presented here are of background-subtracted data.

The background images obtained to the east of Jupiter exhibit an essentially monotonic decrease in intensity with increasing distance from the

planet. Those obtained to the west, however, exhibit a sudden increase in the background intensity across a line on the Jupiter side of the field roughly parallel to the projected Jovian rotation axis (cf. Fig. 1f). This discontinuity appears to be the result of an internal reflection from the telescope tertiary mirror which in its stowed position introduces an east-west asymmetry into the scattering characteristics of the telescope.

Another characteristic of background images obtained on both sides of the planet is lower intensity at the southern edge of the field than at the north. This does not appear to be due to the flat field response of the image tube, which is known not to have variations in the red exceeding 10% (Stockton, private communication). There are two possibilities. One is that the north-south variation results from non-uniform scattering of the Jovian background radiation. In this case the effect on the sodium images will be completely removed in the process of background subtraction. The second possibility is that the effect results from non-uniform system transmission affecting the sodium as well as the background radiation. Indeed, as noted below, many of our background-subtracted images show generally brighter emission to the north of Io along a north-south line passing through the satellite. However, others show brighter emission to the south and some show no appreciable asymmetry at all along this line (e.g., Figure 7d). We conclude that the north-south variations in the brightness of the sodium cloud at Io's distance from Jupiter in our data reflect primarily previously observed effects (e.g., Trafton, 1977, 1980), discussed below, of the oscillating plasma torus.

We made no attempt to observe photometric standards during these observations. However, it is possible to obtain a rough estimate of the absolute brightness levels of data that fell within the reproducible range of our intensity calibration curves. We assume that the brightest [S II] λ6731 emission in the images discussed by Pilcher et al. (1981) is 800 R, a value in accord with photometric observations of this line (Trauger et al., 1980; Brown and Shemansky, 1982). Inspection of contour plots of the brightest of these data, corrected for the system spatial transmission function, yields a corrected-relative-intensity (CRI)-to-Rayleighs conversion factor of ~1.1. Allowance for the fact that the sulfur exposures were 10 minutes while those for sodium were only 3 minutes leads to a CRI-to-Rayleighs conversion factor of ~4 for the sodium data. (The conversion factor for uncorrected data varies across the

field of view.) It should be kept in mind, however, that for uncorrected relative intensity values above ~400 (CRI values above ~1600), the intensity scale may be substantially non-linear. Accordingly, CRI values much above ~1600 should be regarded as having little quantitative significance.

III. OBSERVATIONAL RESULTS

The observations discussed here were obtained in 1980 and 1981. The dates and times are given in Table I. The aspect of the data we will address in this paper is the presence of directional features, defined as elongated features whose symmetry axes are generally inclined to the direction expected for features in Io's orbital plane. We will further confine our discussion to features directed away from Jupiter as projected onto the plane of the sky. Since these features usually extend beyond Io's orbital distance of 5.9 R_J, they must comprise sodium whose initial speed at 5.9 R_J is greater than Io's orbital speed. Features directed inward toward Jupiter, also present in our data, may result from ejection in other directions and at lower velocities.

Outward directional features, inclined both to the north and south of Io's orbital plane, were detected on almost every occasion on which we observed in 1980, but less often in 1981. On one occasion, January 6 UT, 1980, a feature was seen to change its direction from southward to northward. Three images of this feature are illustrated in Figures 3 and 4. (In these observations the variation in system transmission across the field-of-view resulted in severe attenuation of sodium emission inward of Io.) In the first observation shown in Figures 3a and 4a, the directional feature is inclined slightly toward the south. Less than two hours later (Figures 3b and 4b), the feature was inclined slightly toward the north. Approximately another two hours later (Figures 3c and 4c), the observed feature's axis of symmetry was inclined even farther to the north. A background image obtained as part of this sequence is shown in Figure 3d. Any instrumental effect associated with the weak north-south intensity gradient present in the background cannot be responsible for the much stronger north-south variations manifested by the directional features. Other images obtained in this sequence showed the sodium emission inward of Io's position to be concentrated to the north of Io's orbital plane throughout the ~ 4-hour interval of observations. The directionality of the final northward feature shown in Figures 3c and 4c may therefore be somewhat exagerated, since an image showing all of the sodium emission present at that time would likely show a broad region of brighter emission to the north.

The general morphology of the feature observed in this sequence, particularly as seen in Figures 3a and 4a, is not unusual. In Figure 5 we show a sim-

ilar feature, although inclined to the north, observed more than a year later. We therefore proceed under the assumption that the change in inclination of the apparent symmetry axis illustrated in Figures 3 and 4 is real and characteristic in general of the process forming the directional features. This change in inclination, and the more general observation that features may be directed to either side of Io's orbital plane, indicate that the features are not associated with any single region on Io's solid surface. Rather, a process involving interaction with the plasma torus, which oscillates north-south with respect to Io, is suggested. We discuss such a model in Section IV.

A large increase in the brightness of the sodium cloud around Io and in the general region of the directional features was observed in February 1980. A group of images from the second night of the four-day interval in that month during which we acquired data was shown in Figure 1. In Figure 6 we show transmission-corrected contour plots corresponding to three of those images. Although of much higher intensity, the directional features observed during this period share morphological characteristics with some of the rest of the data. The directional feature in Figures 1 and 6 is toward the north and exhibits a narrow core embedded in more diffuse emission. This latter characteristic is also shown weakly, and at much lower brightness, in the image illustrated in Figures 3c and 4c. The emission on the Jupiter side of Io is centered on the projection of the leading portion of Io's orbit onto the plane of the sky (cf. Fig. 6). This is generally consistent with the description of the region-B cloud developed in previous imaging studies (Murcray and Goody, 1978; Goldberg et al. 1980; cf. review by Pilcher and Strobel, 1982). There is also an overall asymmetry to the sodium cloud along a north/south line passing through Io, as discussed above, that is best seen in the contour maps of Figure 6. In both this case and that illustrated in Figure 4, higher emission intensities are present to the north. Since all of these data were acquired while Io was at northerly magnetic latitudes, this asymmetry is likely an effect of electron impact ionization of sodium in the plasma torus which was predominantly to the south of Io. This asymmetry, which was first observed and discussed by Trafton and Macy (1975; Trafton, 1977, 1980), has since been reported by other observers (Münch and Bergstralh 1977; Murcray and Goody 1978; Pilcher and Schempp 1979).

In Figure 7 we show three images acquired on the fourth night of the period of enhanced sodium emission around Io. The feature in this case is much narrower and directed away from Jupiter toward the south at an inclination on the plane of the sky roughly equal and opposite to that of Figures 1 and 6. In Figure 7, however, the feature appears to be displaced: its extension across the occulting disk does not cross the disk's center, i.e., Io's position. The displacement at Io's radial distance from Jupiter is ~5 arcseconds north. The feature in Figure 7 is also distinctly non-linear. The inclination of the region B cloud, shown projected toward Jupiter most clearly in the contour plot of Figure 7d, does not follow the leading portion of Io's orbit as it does in Figure 6. Explanations for this inclination, as well as an analysis of other information on region B contained in our data, are beyond the desired scope of this paper. Two additional examples of southward directional features are shown in Figure 8.

The evidence that the sodium emission intensity was significantly enhanced for the entire four day period that data were obtained in February 1980 cannot be attributed to geometrical effects such as variations in Io's orbital phase angle. Nor does it appear to be due to photographic or instrumental effects, since the photographic densities of the background images obtained during February are similar to those of background images from January and from later observations at comparable zenocentric distances. Our observation of only one period of enhanced emission, and the fact that in other studies of essentially the same region of circum-Io space no such period has been observed (Murcray and Goody, 1978; Goldberg et al. 1980), indicate that the enhancement is a relatively infrequent occurence. The absence of enhanced emission in the data of Bergstralh et al. (1975, 1977) may be further indication. It may, however, reflect the fact that the small Io-centered region observed by Bergstralh et al. (which is completely obscured by our occulting disc) is dominated by sodium ejected from Io at velocities lower than those necessary for directional feature formation. These lower velocity components may be less affected by the processes responsible for enhancing the high velocity sodium seen in the directional features. A final point to note here is that images of the plasma torus obtained in the light of [SII] λ6716 on the same nights in February that the enhanced directional features were observed showed no unusual characteristics, indicating that a change in plasma properties was probably not responsible for the increased intensity. If this reasoning is correct, then the rate of sodium

escape from Io during this period at the moderate to high velocities required to populate the observed cloud (see Section IV) must have been anomalously high.

As noted above, observations of both northward and southward directional features, and the one case of a feature that changed its orientation from south to north, suggest that a process involving the plasma torus, which oscillates about the satellite plane, is involved in the formation of the directional features. To test this suggestion we divided all of our observations into three categories: those showing a northward directional feature, those showing a southward feature, and those not showing a directional feature. We show the results of this categorization in Figure 9 plotted with respect to the magnetic longitude of Io at the time of observation. It can be seen that all of the northward directional features were observed when Io was between 170 and 360 degrees magnetic longitude. If the observation of one very weak northward feature which faded during the observation is excluded (the data of April 13 UT, 1981), then all the remaining northward features were observed at Io magnetic longitudes between 170 and 300 degrees. Southward features were almost entirely restricted to longitudes outside this range. On two occasions features disappeared during an observing period, and on one occasion, discussed at length above, a feature changed its direction. The data in Figure 9 indicate that the north-south orientation of the directional features is correlated with the magnetic longitude of Io, and that southward features seem to fade or change to northward features for Io magnetic longitudes of about 150 to 160 degrees.

IV. ANALYSIS

We will confine our analysis here to an interpretation of the characteristics of the directional features, defined at the beginning of Section III as those features both inclined to the direction expected for features in Io's orbital plane and projected onto the plane of the sky in the direction away from Jupiter. The bright region-B sodium cloud and the occasional peculiar sodium structural features visible inside of Io's orbit in some of the observations will not be analyzed here.

The implication of the variation with magnetic longitude shown in Figure 9 is that the features would appear to a terrestrial observer to oscillate north and south of the satellite orbital plane with a period of about 13 hours, the orbital period of Io relative to Jupiter's magnetic field. This inferred oscillation indicates that the features are not produced by some active local sodium source on the satellite's surface. It seems more likely that the oscillation results from the modulation of the sodium cloud density near the satellite plane introduced by the time-dependent lifetime of sodium in the oscillating plasma torus. This is the main idea to be pursued in this analysis.

The lifetime of a sodium atom in the Io plasma torus is determined primarily by the rate of impact ionization by plasma torus electrons. The spatial variation of this lifetime is shown in Figure 10 (Smyth, 1983). Along the vertical oscillation of Io, also shown in Figure 10, the lifetime of sodium is small and varies between about one and four hours. Because of this oscillation, it is possible for sodium atoms ejected from Io with a significant northward velocity component to traverse a region of quite different sodium lifetime than atoms ejected simultaneously to the south. An atom ejected to the north when Io is at the northernmost extreme of its oscillation, for example, will enter a region of comparatively long lifetime, while one ejected simultaneously to the south is likely to be ionized relatively quickly. This difference will lead to a significant north-south time-dependent asymmetry in the sodium cloud density outside of Io's orbit (the region of interest for the directional features) if the atoms have speeds within a certain range so as to move in proper phase with the torus' oscillations. If the speeds are too small, the atoms will require half an oscillation period or more to move a significant distance in the plasma torus, and the lifetime histories for the north and south sodium will have

similar time-averaged values. If the speeds are too large, the north and south sodium will again have similar lifetime histories since neither will spend enough time in the torus to be significantly affected. If the directional features are to be explained in terms of the oscillating sink, the relevant sodium source must involve only atoms having an intermediate range of initial speeds.

To define better this intermediate range, one can use the criterion that the initial velocities of sodium atoms relative to the satellite must be large enough to at least populate the circular viewing window in a time interval approximately one-quarter as long as the 13 hour oscillation period of the plasma torus with respect to Io. Several relevant orbit trajectories are shown in Figure 11 projected upon the sky plane for the observational geometry of Plate 1076a (see Figures 3c and 4c). In both Figures 11a and 11b, the three different trajectories correspond to initial velocity vectors that are inclined 30 degrees above the satellite plane and have initial speeds relative to Io of 6, 10 and 20 km sec^{-1}. The components of the initial velocity vectors in the satellite plane are directed along the orbital motion of Io for Figure 11a and along the anti-Jupiter direction for Figure 11b. These trajectories suggest that initial speeds of approximately 20 km sec^{-1} satisfy the speed criterion, with slightly larger speeds acceptable for the initial velocity direction of Figure 11a and slightly smaller speeds acceptable for that of Figure 11b. Initial speeds of 10 km sec^{-1} or less are too slow and more than 30 km sec^{-1} (not shown in Figure 11) are too fast.

With the speed range defined, we used the Io sodium cloud model of Smyth (1983), recently improved to include the oscillating plasma torus sink for sodium (Smyth and Combi, 1983; also see Smyth, 1983), to perform several exploratory calculations. The observational sequence shown in Figures 3 and 4 was selected for a model-data comparison, since it provides the potentially diagnostic observation of a change in feature direction from south to north (these observations are also illustrated as the January 6 UT, 1980 data in Figure 9). In our first exploratory model calculations, we assumed the sodium to be ejected at 20 km sec^{-1} from the trailing hemisphere exobase of the satellite (excluding a stagnation region centered on the trailing hemisphere apex). Our choice of the trailing hemisphere to be the source region was motivated by the thought that the directional features may result from an interaction between Io and the corotating magnetospheric plasma which most directly im-

pinges on the satellite's trailing hemisphere. At the assumed velocity of 20 km sec^{-1}, solar radiation pressure effects can be ignored. The initial velocity vectors on the exobase were not radially directed, but were arranged in a cylindrically symmetric fashion about the direction of Io's orbital motion and inclined by an angle α above the forward-directed tangent vector to the exobase surface. The angle α was assumed to have small values, mostly between 0 and 20 degrees, as suggested by line profile studies (cf. Section I) which showed sodium to be ejected in the forward direction and by the momentum direction of the magnetospheric plasma moving past Io.

The exploratory model results for the three observations of Figures 3 and 4 did not produce distinct directional features. Furthermore, the north-south asymmetry in the calculated sodium intensity on the sky plane was toward the south for both Plates 1069c and 1073a and only weakly toward the north for Plate 1076a. This is in disagreement not only with this particular sequence of observations, but also with the general trend of feature directionality with Io magnetic longitude illustrated in Figure 9. It can be seen from this figure and, for example, Figures 1 and 6, that Plate 1076a was acquired at an Io magnetic longitude well into the range in which strongly northward directed features have been observed. The quite weak northward enhancement calculated for this plate thus seems to be generally inconsistent with the data. The situation was not significantly improved when we considered a severe system III magnetic longitude dependence to the electron impact ionization lifetime of sodium in the plasma torus, nor when we included an initial speed dispersion for the sodium atoms. This suggests that the north-south orientations of the directional features are controlled more by the general oscillatory nature of the plasma torus than by the fine details of the spatial lifetime structure of sodium. It also suggests that the orientations of the initial velocity vectors chosen for the exploratory calculations are not appropriate to explain the directional features.

In order to search more effectively for the proper orientations of the initial velocity vectors for the sodium atoms, we developed a correlation technique and applied it to the observations of Figures 3 and 4. Our aim was to correlate the initial velocity directions of sodium atoms with their resulting contributions to the D-line intensity in the observing window. To cover all possible directions, it was sufficient to consider a set of initial velocity

vectors that were directed radially and isotropically from Io's exobase. This approach is valid for the relatively large initial speeds of 20 km sec^{-1} under consideration, since the path of an atom leaving Io at such a speed is almost totally dependent upon its initial velocity direction and almost totally independent of its initial location on the exobase. For purposes of this study, the exobase of Io (assumed to be 2600 km in radius) was divided into 613 north-south pairs of points, each pair comprising two equal areas arranged symmetrically with respect to the equator. The central latitudes and longitude of each pair were taken to be the coordinates of radial ejection of sodium atoms from the exobase. The Io sodium cloud model was then used to calculate the space-time D_2-line intensity contribution along each north-south pair of trajectories for an initial speed of 20 km sec^{-1} and the magnetic and viewing geometries corresponding to the observations of Figures 3 and 4.

For the purpose of this study, we defined upper and lower windows in the main observing window as shown in Figure 12. For each trajectory pair, we calculated the cumulative D_2-line intensity contributions to the upper window I_U and the lower window I_L. We found that a 20-hour flight time was the maximum we need consider. We also computed the intensity ratio given by

$$R = \frac{I_U}{I_L} . \qquad (1)$$

If R is greater than one, the trajectory pair contributes primarily to a northern enhancement in the D-line intensity. If R is less than one, the enhancement is to the south. For each trajectory pair, the value of R can therefore be associated with two angles, the ejection longitude and the absolute ejection latitude. Since the atoms are assumed to be ejected radially, these angles describe the initial velocity directions of the pair. Our results for all of the 613 north-south pairs that make a contribution to the intensities in the upper and lower viewing windows are summarized in Figure 13. We have followed here the normal longitude convention in which the sub-Jupiter point is at 0° and the apex of motion is at 90°. The three parts of Figure 13 correspond to the geometries of the three observations of Figures 3 and 4. Values of R greater than unity have been displayed as three sizes of the letter N, while corresponding values of R^{-1} have been displayed as the same three sizes of the letter S. The large N (or S) symbols correspond to values of R (or R^{-1}) larger than 2, the intermediate N (or S) symbols to values between 2.0 and 1.5, and the small N (or S) symbols to values between 1.5 and 1.0.

The results of the correlation study in Figure 13 are striking. These results show that sodium atoms with initial velocity vectors directed radially outward and somewhat normal to Io's orbital motion (i.e., 180° ejection longitude) have the correct orientation to explain generally the south-to-north changes that occur in the directional features shown in Figures 3 and 4. Results in Figure 13 also confirm our earlier exploratory model conclusions that sodium atoms ejected with initial velocity vectors directed nearly parallel to Io's orbital motion produce intensity patterns that are too bright in the south (see the large S's at low latitudes and longitudes less than 90° in Figure 13).

The spatial morphology of the sodium D_2-line intensity seen on the sky plane through the viewing window, produced by 20 km sec^{-1} sodium atoms directed at nearly right angles to Io's orbital motion, is therefore the appropriate situation to be explored. To accomplish this we used the Io sodium cloud model with the ejection of sodium atoms from Io restricted to the band illustrated in Figure 14. The band is centered on the great circle that is normal to Io's orbital motion direction and extends about 20 degrees toward the leading and trailing hemisphere apexes. In the model calculation 456 trajectories, corresponding to atoms emitted from equal areas distributed symmetrically around the band, were used to simulate the escape of sodium from Io. For equal sodium flux from all areas and a value for the ejection angle α of 90 degrees (i.e., radial ejection), the calculated D_2 intensity distributions corresponding to the observational geometries of Figures 3 and 4 are shown in Figure 15. Note that in Figure 15 the general intensity pattern calculated from the model changes from slightly south to north in phase with the observations. The model calculation thus exhibits the correct dependence on the magnetic longitude of Io, but lacks the distinct spatial character of the observed features.

The extreme northern enhancement of the calculated sodium intensity for Plate 1076a in Figure 15 is to be expected and may be understood as follows. As discussed above, sodium atoms ejected from Io to the north at the intermediate velocities in question have a decided lifetime advantage if they are ejected when Io is near the northern extreme of its oscillation with respect to the plasma (cf. Fig. 10). A northern enhancement in the sodium cloud density then results. This is the case (see Fig. 13c) for Plate 1076a (Figures 3c and 4c), which was acquired when Io was at 9.2° north magnetic latitude and had been at high northern magnetic latitudes for the preceding 2-3 hours. A cor-

responding southern enhancement results in the calculations when Io is assumed to be near the southern extreme of its oscillation. The overall effect in the model is a broadening of the emission distribution to the north or south with a corresponding loss of specific directionality.

To obtain more pronounced and definitely directional features in the model, as are seen in the observations, this high latitude lifetime advantage must be compensated for by an enhancement of the escape flux of sodium from low latitudes. We therefore examined the consequences of a latitude-weighted distribution in which the flux of sodium ϕ from the band ejection region is described by the expression

$$\phi = \phi_0 (1 - f|\sin \Phi|), \tag{2}$$

where ϕ_0 is the flux on the band at the equator, Φ is the angle measured from the equator along a line parallel to the great circle that is the center of the band ejection region, and f is a reduction factor chosen from a model-data comparison to have a value of 0.7.

The results from this latitude-weighted band ejection model, calculated for the observing geometry of Plate 1069c (Figures 3a and 4a), are shown in Figure 16 for several values of the ejection angle α and an initial speed of 20 km sec^{-1}. The results for ejection angles of 75°, 90°, and 105° show a directional character to the emission outward of Io that is more consistent with the observations than the unweighted results. The intensity distribution calculated for 105° most clearly shows southward directionality, in accord with the corresponding observation.

For ejection angles of 60 degrees and smaller, a more prominent southward directional feature forms that exhibits neither the correct spatial morphology nor the observed Io magnetic longitude phase relation shown in Figure 9. This is consistent with our earlier exploratory runs and with the correlation results of Figure 13. For ejection angles of 120° and larger, it becomes increasingly difficult to produce significant directionality. This occurs for two reasons. First, the lower resultant orbital velocities of atoms ejected on these trajectories result in their not traveling as far outside of Io's orbit as atoms ejected at smaller angles, and therefore not being seen as far from Io's position on the plane of the sky. Second, at these smaller distances from

Jupiter, the atoms are more readily ionized by the plasma and hence contribute less D-line emission intensity. It therefore appears that the directions of the initial atomic velocity vectors most consistent with the morphologies of the directional features are outward from Io, at approximately right angles to the orbital motion of the satellite, with atomic flux generally decreasing from equator to pole.

The results of model calculations made with this weighted band ejection model for all three of the observations of Figures 3 and 4 are shown in Figure 17. Here we have adopted an ejection angle α of 90° (i.e., radial ejection), although the use of 75° or 105° gives very similar results. The calculated intensity distribution outward of Io is similar in general shape and dependence on Io magnetic longitude to the observations.

Since the directional features in these model calculations result from initial velocity vectors directed outward from Io's orbit within a narrow longitudinal angular range, the question arises as to whether the features could just as well be produced by radial ejection from the trailing hemisphere of Io. This may be possible since radial ejection from the portion of the trailing hemisphere that does not overlap the band region is less able to contribute to intensity within the observing window. There are two reasons for this. First, the atoms on the trajectories that originate on the trailing hemisphere outside the band region lie closer to Io's orbit and hence are more susceptible to ionization by the plasma torus. Second, a significant fraction of these atoms rapidly move inside of Io's orbit and are either lost from the cloud by collision with Jupiter or contribute only to the near-Io region-B cloud. To pursue this idea, we performed calculations in which the trailing hemisphere was divided into 649 equal area segments, from each of which we assumed sodium to be ejected radially at 20 km sec^{-1}. The escape flux ϕ of sodium was enhanced near the equator through the use of a latitudinal distribution given by expression (2) where ϕ_0 is the sodium flux at the equator, Φ is now latitude, and f is a reduction factor chosen again to have a value of 0.7.

Results for all three observations of Figures 3 and 4 are shown in Figure 18. The general spatial morphology of these calculated D_2 intensity contours compares favorably with the observations. For Plate 1069c, however, the calculated feature is not as vertically distinct as in the observation (Figure 4) or as in the band ejection model results (Figure 17). This reduced directionality

is apparent also in the band ejection results of Figure 16 for an ejection angle α of 120 degrees, and reflects the importance of velocity vectors on the forward half of the band ejection region. Any real ejection region centered on the trailing hemisphere of Io would, of course, likely yield some velocity vectors with forward components. This would naturally extend the effective exobase region of ejection beyond the strict geometric boundary adopted in the model. As anticipated, apart from these differences, the spatial intensity morphologies of the features shown in Figure 18 are similar to those calculated for the band ejection and shown in Figure 17.

From examination of the correlation results of Figure 13, one might also ask if the directional features of Figures 3 and 4 could be suitably modeled by radial ejection from the leading hemisphere. This may be possible if ejection from that portion of the leading hemisphere that overlaps half of the band region is sufficiently strong to dilute the intensity contributions of the ejection originating closer to the hemispherical apex, which has been shown earlier to provide a southern enhancement. To examine this situation, we simulated leading hemisphere ejection from the satellite exobase by a procedure corresponding exactly to that adopted for the trailing hemisphere. The model results for all three observations of Figures 3 and 4 are shown in Figure 19. The general change in the direction of the feature from south to north is in the correct sense but can be seen to lag behind the observation (i.e., the direction of the calculated feature advances toward the north too slowly). The north-south character of the feature is also broader than in the observations or the band ejection results (Figure 17). These characteristics result as anticipated, from the southern intensity contributions made by sodium ejected near the apex of the leading hemisphere and around the leading-inner quadrant at low latitudes (see Figure 13). An appropriate variation of atomic flux with longitude that reduced the importance of these atoms could therefore be used to improve the agreement of this variation of the model with the observations. However, the presence of some of these near forward-directed atoms with speeds up to 20 km sec^{-1} has been shown to be required for the proper modeling of the asymmetric skirt of the sodium D-line profile (see the discussion in Section I). In a model that accounts for both the directional features and the D-line profiles, therefore, the directional features may prove to be understandable as the spatial counterpart of the spectral signature given by the asymmetric skirt.

By comparing the estimated brightness levels from Figure 4 with the model results of Figures 17, 18 and 19, we may estimate the satellite equatorial atomic flux ϕ_0 and the total rate of sodium ejection from Io at these velocities. As discussed in Section II, the brightnesses corresponding to the contours plotted in Figure 4 may be estimated (within a factor of 2-3) by means of the rough conversion factor of ~4 from CRI (corrected relative intensity) units to Rayleighs. For the band ejection models of Figure 17, the equatorial flux ϕ_0 required to match the observations is about 2.5×10^9 atoms cm^{-2} sec^{-1} for Plate 1069c and about 2.1×10^9 atoms cm^{-2} sec^{-1} for Plates 1073a and 1076a. Integrating the non-uniform flux distribution over the band region, we find this corresponds to a total satellite source rate between about 1.7 and 2.0×10^{26} atoms sec^{-1}. Only about half of these atoms contribute to the directional features in the viewing window (see Figure 13). For the trailing hemisphere ejection model results of Figure 18, the required equatorial flux is 5×10^9, 3.2×10^9 and 2.7×10^9 atoms cm^{-2} sec^{-1}, respectively, for Plates 1069c, 1073a, and 1076a. This corresponds to a total satellite source rate between about 3.7 and 6.8×10^{26} atoms sec^{-1} for the postulated non-uniform flux distribution over the trailing hemisphere exobase. At most half of this material contributes to the brightness of the directional feature seen in the viewing window. For the leading hemisphere ejection model results of Figure 19, the required equatorial flux is about 1.4×10^9 atoms cm^{-2} sec^{-1} for all three observations. This corresponds to a total satellite source rate of about 1.8×10^{26} atoms sec^{-1} of which slightly more than half may contribute to the directional feature. From these comparisons, we conclude that the source rate required to produce the directional features is of order 10^{26} atoms sec^{-1}.

V. DISCUSSION

The general conclusions that we have derived in the analysis may be stated as follows. The directional features result from the combined effects of a source of high speed (~20 km sec^{-1}) sodium and the oscillating Io-plasma-torus sink for neutral sodium. The Io magnetic longitude at which the computed features in our model change direction with respect to Io's orbital plane is critically dependent on the directions of the initial velocity vectors of the high speed atoms. To account for the observations, these must be directed essentially at right angles to Io's orbital motion. The directionality of the features requires that the flux of sodium escaping from Io generally decrease from equator to pole. The required initial velocity directions are consistent with (1) radial atomic ejection from a band region of narrow longitudinal extent centered on the great circle separating the leading and trailing hemispheres, (2) approximately radial ejection from the trailing hemisphere (possibly extending forward into the leading hemisphere by 20° and possibly with little or no ejection from a region centered on the trailing hemisphere apex), or (3) radial ejection from the leading hemisphere with a substantial decrease in flux toward the apex of motion. The actual sodium source may be distributed over some combination of these regions, as illustrated in Figure 20a.

We have not thus far appealed to any particular physical mechanism to explain the deduced characteristics of the sodium ejection from Io. We note, however, that the required right-angle direction of ejection of sodium from the satellite relative to its orbital motion is exactly the same direction shown to occur for the elastic scattering of neutral atoms from Io by magnetospheric ion impacts (Sieveka, 1983; Sieveka and Johnson, 1984). The near right angle orientation of the neutral atoms follows naturally from the scattering properties of a screened coulomb potential which realistically describes the ion-neutral collisional interaction. This is in marked contrast to the highly forward-peaked scattering which results from hard-sphere interactions. The required single scattering of atoms could occur in an extended neutral corona of the satellite, producing a substantial atomic flux in the 10 to 30 km sec^{-1} velocity range. The corona may be populated by ion sputtering of neutrals from the trailing hemisphere of Io's surface (in the low density atmospheric limit) or exobase (in the high-density atmospheric limit). In addition, somewhat radial

ejection of neutral atoms may be produced directly by sputtering from the trailing hemisphere surface or exobase.

Our conclusions, based on analysis of the directional features together with the calculations of Sieveka (1983) and Sieveka and Johnson (1984), provide direct evidence for a magnetospheric-wind-driven gas escape mechanism. Either the somewhat radially directed sodium atoms expected from sputtering, or the near right angle source of sodium provided by scattering in the corona (or, realistically, a combination of the two) may supply the necessary atoms to explain the directional features. The relative importance of the sputtered and corona sources will depend upon the local properties of the satellite atmosphere (and/or surface) and its interaction with the plasma flow pattern in the vicinity of Io. A simple flow pattern that is suggested by the ejection pattern of Figure 20a is illustrated in Figure 20b. More elaborate plasma flow patterns based upon a two-dimensional electric dipole have been adopted by Ip (1982) and used to argue that such a dynamic coupling of a neutral atmosphere and the corotating plasma can provide a significant source for the neutral clouds in the Jovian system.

Further quantitative study of the directional feature data coupled with calculations of the flux and angular distribution of escaping material from the satellite surface or exobase and from its corona may allow definite conclusions to be drawn as to the presence or absence of a substantial atmosphere on Io. In addition to this information, the indication that the sodium flux is enhanced at the equator may reflect a latitudinal structure in the atmosphere, perhaps produced by volcanic activity near the equator or by colder temperatures nearer the satellite poles. The very strong directionality of some features not analyzed here (see, for example, Figures 1, 6, and 7) may reflect temporal variation in this structure. Observations in which the directional features are weak or absent may also be diagnostic of changes in the magnetospheric properties or satellite atmosphere. Further studies of the directional feature data together with the region-B cloud data (not considered here) are necessary to determine the total source rate of sodium. This is important for understanding the source rates and escape mechanisms operative at Io for other gases such as those containing oxygen and sulfur, the ions of which constitute the bulk of the plasma in Jupiter's inner magnetosphere.

Although the direct evidence deduced from the directional feature data supporting a magnetospheric-wind-driven gas escape mechanism for Io is new, the general subject has been under discussion for several years. Charged-particle sputtering of sodium from Io's surface was first suggested by Matson et al. (1974). Laboratory investigations of ion sputtering from various icy surfaces have subsequently been actively pursued (Brown et al. 1980; Lanzerotti et al. 1982; Brown, Lanzerotti and Johnson, 1982; Johnson et al. 1983) to evaluate the mechanism more quantitatively. Sputtering from the atmosphere of Io by the corotating thermal plasma was also initially discussed by Haff, Watson and Yung (1981) and more recently by Summers, Yung, and Haff (1983). Single-scatter elastic collisions of neutrals with the corotating thermal plasma (i.e., knock-on processes) and charge exchange processes have been discussed by several authors (Brown and Schneider, 1981; Ip, 1982; Brown, Pilcher and Strobel, 1983). The recent efforts of Sieveka (1983) and Sieveka and Johnson (1984) have been more specific and have begun to address these various escape processes collectively and more quantitatively. Additional efforts in this direction should prove to be very valuable in our attempts to understand better the characteristics of the directional features of the sodium cloud.

ACKNOWLEDGMENTS

The authors would like to thank J.S. Morgan for many valuable discussions, and E.M. Sieveka and R.E. Johnson for sharing the results of their ion-neutral-impact calculations prior to publication. This work was supported in part by grants to the University of Hawaii from the Planetary Astronomy, Planetary Atmospheres, and Planetary Geology sections of NASA and from the Solar System Astronomy section of the National Science Foundation, and by grant NASW-3387 to Atmospheric and Environmental Research, Inc. from the Planetary Atmospheres program of NASA. Acknowledgment is also made to the National Center for Atmospheric Research, which is sponsored by the National Science Foundation, for the computer time used in model calculations.

REFERENCES

Bagenal, F., and Sullivan, J. D. 1981, J. Geophys. Res., 86, 8447.

Bergstralh, J. T., Matson, D. L., and Johnson, T. V. 1975, Ap. J. (Letters), 195, L131.

Bergstralh, J. T., Young, J. W., Matson, D. L., and Johnson, T. V. 1977, Ap. J. (Letters), 211, L51.

Bridge, H. S., Sullivan. J. D., and Bagenal, F. 1980, Private communications.

Brown, R. A. 1974, in IAU Symposium 65, Exploration of the Planetary System, ed. A. Woszczyk and C. Iwaniszewska (Dordrecht: Reidel), pp. 527-531.

Brown, R. A., and Chaffee, Jr., F. H. 1974, Ap. J. (Letters), 187, L125.

Brown, R. A., and Shemansky, D. E. 1982, Ap. J., 263, 433.

Brown, R. A.,. Pilcher, C. B, and Strobel, D. F. 1983, in Physics of the Jovian Magnetosphere, ed. A. J. Dessler, (New York: Cambridge University Press), pp. 197-225.

Brown, R. A., and Schneider, N. M. 1981, Icarus, 48, 519.

Brown, W. L., Augustyniak, W. M., Brody, E., Cooper, B., Evatt, R., and Johnson, R. E. 1980, Nucl. Inst. & Meth., 170, 321.

Brown, W. L., Lanzerotti, L. J., and Johnson, R. E. 1982, Science, 218, 525.

Carlson, R. W., Matson, D. L., Johnson, T. V., and Bergstralh, J. T. 1978, Ap. J., 223, 1082.

Goldberg, B. A., Mekler, Yu., Carlson, R. W., Johnson, T. V., and Matson, D. L. 1980, Icarus, 44, 305.

Haff, P. K., Watson, C. C., and Yung, Yuk L. 1981, J. Geophys. Res., 86, 6933.

Ip, W.-H. 1982, Ap. J., 262, 780.

Johnson, R. E., Garrett, J. W., Boring, J. W., Barton, L. A., and Brown, W. L. 1983, Preprint.

Lanzerotti, L. J., Brown, W. L., Augustyniak, W. M., Johnson, R. E., and Armstrong, T. P. 1982, Ap. J., 259, 920.

Matson, D. L., Goldberg, B. A., Johnson, T. V., and Carlson, R. W. 1978, Science, 199, 531.

Matson, D. L., Johnson, T. V., and Fanale, F. P. 1974, Ap. J. (Letters), 192, L43.

McFarland, R. H. 1965, Phys. Rev., 139, A40.

McFarland, R. H., and Kinney, J. D. 1965, Phys. Rev., 137, A1058.

Mekler, Yu., and Eviatar, A. 1974, Ap. J. (Letters), 193, L151.

Münch, G., and Bergstralh, J. T. 1977, Publ. Astron. Soc. Pacific, 89, 232.

Murcray, F. J. 1978, Ph.D. Thesis, Department of Physics, Harvard University.

Murcray, F. J., and Goody, R. M. 1978, Ap. J., 226, 327.

Pilcher, C. B. 1980, Science, 207, 181.

Pilcher, C. B., Morgan, J. S., Fertel, J. H., and Avis, C. C. 1981, Bull. Amer. Astron. Soc., 13, 731.

Pilcher, C. B., and Schempp, W. V. 1979, Icarus, 38, 1.

Pilcher, C. B., and Strobel, D. F. 1982, in Satellites of Jupiter, ed. D. Morrison (Tucson: University of Arizona Press), pp. 807-845.

Scudder, J. D., Sittler, Jr., E. C., and Bridge, H. S. 1981, J. Geophys. Res., 86, 8157.

Shemansky, D. E. 1980, Private communication.

Sieveka, E. M. 1983, Ph.D. Thesis, Department of Nuclear Engineering and Engineering Physics, University of Virginia.

Sieveka, E. M., and Johnson, R. E. 1984, Submitted to Ap. J.

Smyth, W. H. 1983, Ap. J., 264, 708.

Smyth, W. H., and Combi, M. R. 1983, Bull. AAS, 15, 810.

Smyth, W. H., and McElroy, M. B. 1977, Planet. Space Sci., 25, 415.

Smyth, W. H., and McElroy, M. B. 1978, Ap. J., 226, 336.

Summers, M. E., Yung, Yuk L., and Haff, P. K. 1983, Nature, 304, 710.

Trafton, L. 1975, Ap. J. (Letters), 202, L107.

Trafton, L. 1977, Ap. J., 215, 960.

Trafton, L. 1980, Icarus, 44, 318.

Trafton, L., and Macy, Jr., W. 1975, Ap. J. (Letters), 202, L155.

Trafton, L., and Macy, Jr., W. 1977, Ap. J., 215, 971.

Trafton, L., and Macy, W. 1978, Icarus, 33, 322.

Trafton, L., Parkinson, T., and Macy, W. 1974, Ap. J. (Letters), 190, L85.

Trauger, J. T., Münch, G., and Roesler, F. L. 1980, Ap. J., 236, 1035.

Trauger, J. T. 1980, Private communication.

Wehinger, P. A., and Wyckoff, S. 1974, IAU Circ., 2701.

Zapesochnyi, I. P., and Aleksakhin, I.S. 1968, Zh. Eksp. Teor. Fiz., 55, 76. [Also, Soviet Physics, JETP, 28, 41, 1969.]

Table I

Date(UT)		Plate Numbers	Start Time (UT)	End Time (UT)
1980	Jan. 5	1065,1066	1207	1303
	Jan. 6	1069-1076	1014	1424
	Jan. 7	1079	1144	1153
	Feb. 5	1083	842	852
	Feb. 6	1088-1091	823	1000
	Feb. 7	1095-1098	946	1119
	Feb. 8	1103-1105	836	947
	Apr. 21	1191-1194	922	1050
	Apr. 22	1203	921	933
1981	Mar. 10	1446-1454	722	1439
	Mar. 11	1455,1456	821	850
	Mar. 11	1459-1462	1101	1323
	Mar. 12	1465,1466	833	911
	Mar. 12	1471,1472	1351	1420
	Mar. 13	1473,1474	700	730
	Apr. 9	1838-1841	1016	1203
	Apr. 10	1845,1846	909	1021
	Apr. 13	1862-1869	551	1004

FIGURE CAPTIONS

Figure 1. Photographs of plates of the sodium emission around Io obtained on 1980 Feb. 6 between 823 and 909 UT. Each image is 110 arcseconds (5.0 R_J) in diameter. Io's image is centered on the 14-arcsecond occulting disk that appears as a bright spot in the center of each negative image. North is up and east is to the left. Jupiter is to the left, Io being essentially at western elongation when these images were acquired (see Fig. 6). The sequence a - f corresponds to a sequence of increasing filter tilt angle from 1° to 6° in 1° increments. The differences between images are explained in the text. The vertical intensity discontinuity near the left edge of each image, seen best in images c - f, is an artifact caused by scattering within the telescope. The directional feature, evident in images a - d, extends from the occulting disk toward the upper right to the margin of the field. Image f is a measurement of the background which was used in the reduction of images a - d (see text).

Figure 2. (a) The calculated instrumental spatial transmission function for sodium D_2-line radiation corresponding to the image of Fig. 1b, which was acquired at a filter tilt angle of 2°; (b) Same as a, but for the image of Fig. 1c, which was acquired at a filter tilt angle of 3°; (c) Same as a, but for the image of Fig. 1d, which was acquired at a filter tile angle of 4°.

Figure 3. Photographs of plates obtained on 1980 Jan. 6 UT. North is up and east is to the left. Jupiter is to the right. Additional details are given in the caption to Fig. 1. Details regarding images a - c, which show the directional feature, are given in the legends of Fig. 4. In these images, all of which were obtained at a filter tilt angle of 2-1/2°, the sodium emission inward of Io (to the right of the occulting disk) was severely attenuated owing to the spatially non-uniform system transmission. Image d is a background image obtained 12 minutes after image b at a filter tilt angle of 8°.

Figure 4. Contour plots of the images shown in Figures 3a - c. North is up and east is to the left. Jupiter, Io's orbit, and Io's position at the time of the observation are illustrated. The background has been subtracted and the resulting images corrected for the system spatial transmission function as described in the text. Inward of Io's position the spatial transmission function for these observations is so low that little sodium radiation is transmitted. The contour values in corrected-relative-intensity (CRI) units are as follows: (a) 65, 112, 150, 250, 450, 750, 1100; (b) 65, 90, 200, 500, 1200; (c) 65, 100, 190, 400, 800, 1400. For a rough conversion from CRI units to Rayleighs, multiply by a factor of 4.

Figure 5. Photographs of images obtained on 1981 April 10 between 909 and 916 UT. Jupiter is to the right (west). See the caption to Fig. 1 for additional details. The unocculted image of Ganymede, to the lower right of the occulting disk, is surrounded by rings of scattered light, one of which transects the directional feature.

Figure 6. Contour plots of the images shown in Figures 1b - d. The format and data processing are as described in the caption to Fig. 4. The contour values in CRI units are as follows: (a) 65, 150, 250, 375, 625, 1000, 1750, 3500, 5000, 6500; (b) 65, 150, 250, 375, 625, 1000, 1750, 3500, 5000; (c) 65, 150, 250, 375, 625, 1000, 1750, 3500, 5000. As discussed in the text, CRI values in excess of ~1600 should be regarded as having only qualitative significance. The CRI values of these three images are in good agreement despite substantial differences between the uncorrected intensity levels.

Figure 7. (a-c) Photograph of a plate obtained on 1980 Feb. 8 between 836 and 850 UT. Jupiter is to the left (east). See the caption to Fig. 1 for additional details; (d) A contour plot of the image shown in b. The format and data processing are as described in the caption to Fig. 4. The contour values in CRI units are as follows: 65, 100, 150, 250, 375, 625, 1250, 2500, 5000. CRI values above ~1600 should be regarded as having only qualitative significance. Multiplication by a factor of 4 roughly converts lower CRI values to Rayleighs.

Figure 8. Photographs of images obtained on 1981 Mar. 11 UT (a) and 1981 Apr. 9 UT (b) showing southward directional features. Jupiter is to the right in a and to the left in b. See the caption to Fig. 1 for additional details.

Figure 9. Classification of directional features as a function of Io's magnetic longitude at the time of the observations. Observed northward features are plotted at the top, southward features at the bottom, and null observations (no feature) in the center. Observations at overlapping longitudes have been displaced vertically for clarity. Observations from 1980 are plotted above those from 1981. Solid lines connect data points corresponding to a continuous series of observations on a single night. A dashed line connects the points corresponding to two observations obtained ~3 hours apart on March 11 UT, 1981. The dotted line partially used for the data of April 13 UT, 1981, is meant only to call attention to the fact that during these observations Io passed through 0° magnetic longitude, and the plotted points therefore appear separated in the figure, as do the points for March 11 UT, 1981.

Figure 10. Sodium Electron Impact Ionization Lifetime in the Io Plasma Torus. The lifetime calculation is based upon the cross-sections measured by McFarland (1965), McFarland and Kinney (1965) and Zapesochnyi and Aleksakhin (1968), Voyager 1 in situ measurements of the plasma density (Bridge, Sullivan and Bagenal, 1980; Bagenal and Sullivan, 1981), and Voyager 1 UVS (Shemansky, 1980) and in situ measurements (Scudder, Sittler and Bridge, 1981) for the electron temperature. The two-dimensional common temperature model of Bagenal and Sullivan (1981) was selected to describe the electron density.

Figure 11. Orbit trajectories for Different Initial Velocities. The initial speed and total flight time for each trajectory are given, with one-hour tick marks indicated. Also shown to scale on the sky plane are Jupiter, Io's orbit, Io at 121° orbital phase, and the outer boundary of the observing window which is centered on Io. See text for orientation of the initial velocity vectors.

Figure 12. Correlation Study for the Directional Feature. The upper and lower segments of the viewing window adopted in the correlation study are shown to scale with Jupiter and Io's orbit, for the satellite at eastern elongation.

Figure 13. Results of a Study of the Correlation Between the Angle at which Sodium Atoms are Ejected from Io and the North-South Orientation of the Resulting Region of Enhanced D-line Emission. Three sizes of N or S, corresponding to more northerly or southerly intensity enhancements in the upper (northern) and lower (southern) viewing windows defined in Fig. 12 are shown on a latitude-longitude plane. The location of a point on this plane corresponds to the location on Io's exobase from which the atoms producing the indicated enhancement would be ejected. The ejection of atoms from the exobase is assumed to be radial at 20 km sec^{-1}. See the text for more quantitative details.

Figure 14. Band Ejection Model. The directions of the initial velocity vectors for sodium atoms ejected from the band region, which is oriented symmetrically about the direction of Io's orbital motion, is illustrated. The angle α can be adjusted to simulate both forward and backward ejection.

Figure 15. Results of Unweighted Band Ejection Model Calculations. The calculated D_2-line intensity contours corresponding to the three observations of Figures 3 and 4 are shown. The spacings of the contours are the same as those of Figure 4, and the flux of atoms from Io has been adjusted to yield approximately the absolute intensities estimated from the observations.

Figure 16. Results of Latitude-Weighted Band Ejection Model Calculations. The D_2-line intensity contours for Plate 1069a (Figure 4a) are shown for five values of the ejection angle α. The contour levels were determined as described in the caption to Fig. 15.

Figure 17. Results of Latitude-Weighted Band Ejection Model Calculations. See the caption to Fig. 15.

Figure 18. Results of Latitude-Weighted Trailing Hemisphere Model Calculations. See the caption to Fig. 15.

Figure 19. Results of Latitude-Weighted Leading Hemisphere Model Calculations. See the caption to Fig. 15.

Figure 20. Magnetospheric-Wind-Driven Gas Escape from Io. (a) The arrows depict the pattern of atomic ejection vectors from Io inferred in this paper to account for the directional features. The most important ejection directions, inferred to be the primary source of sodium for the directional features, are shown in heavier shading for the case of radial atom ejection from Io. The essential character of this primary source is its near orthogonal ejection direction with respect to the satellite motion, and need not necessarily be identified directly with a specific region of the exobase surface as depicted. (b) A simple plasma flow pattern past Io that might produce the ejection pattern in a by ion-neutral interactions is shown.

Carl B. Pilcher*
Institute for Astronomy
University of Hawaii
Honolulu, Hawaii 96822

William H. Smyth
Atmospheric and Environmental Research, Inc.
840 Memorial Drive
Cambridge, Massachusetts 02139

Michael R. Combi
Atmospheric and Environmental Research, Inc.
840 Memorial Drive
Cambridge, Massachusetts 02139

Jeanne H. Fertel
Institute for Astronomy
University of Hawaii
Honolulu, Hawaii 96822

*Address until July 1984

Institut Für Astronomie
Universitäts-Sternwaer
Türkenschanzstrasser 17
A-1180 Vienna, Austria

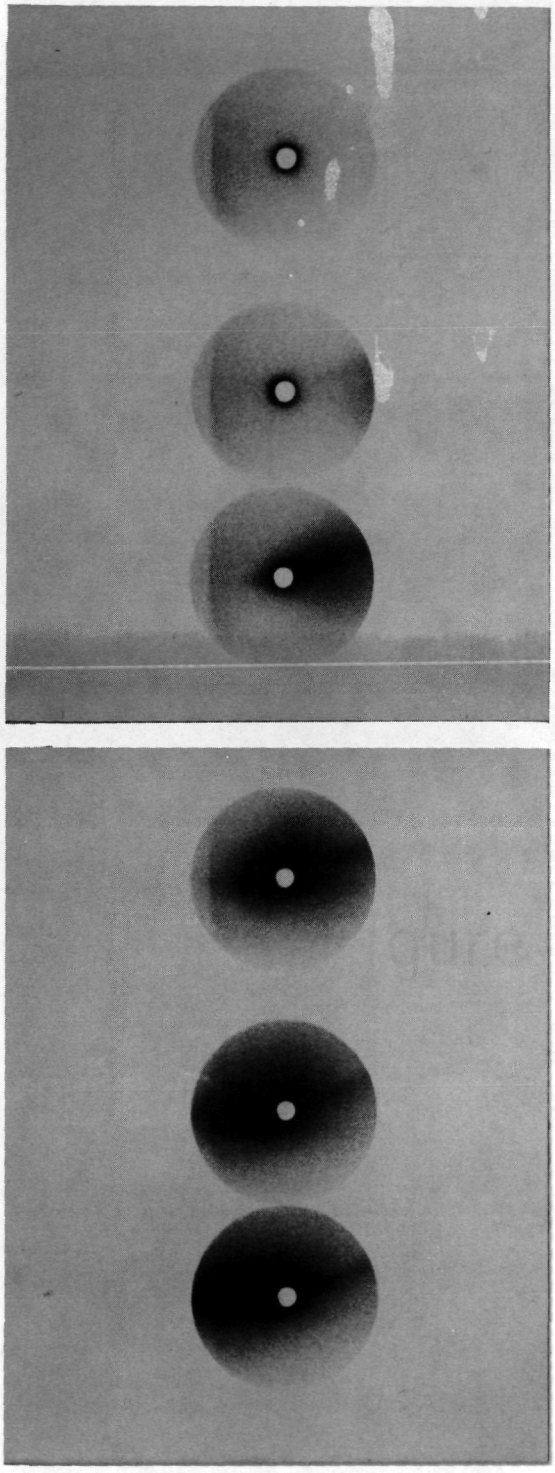

(f) 1089c

(e) 1089b

(d) 1089a

(c) 1088c

(b) 1088b

(a) 1088a

Figure 1

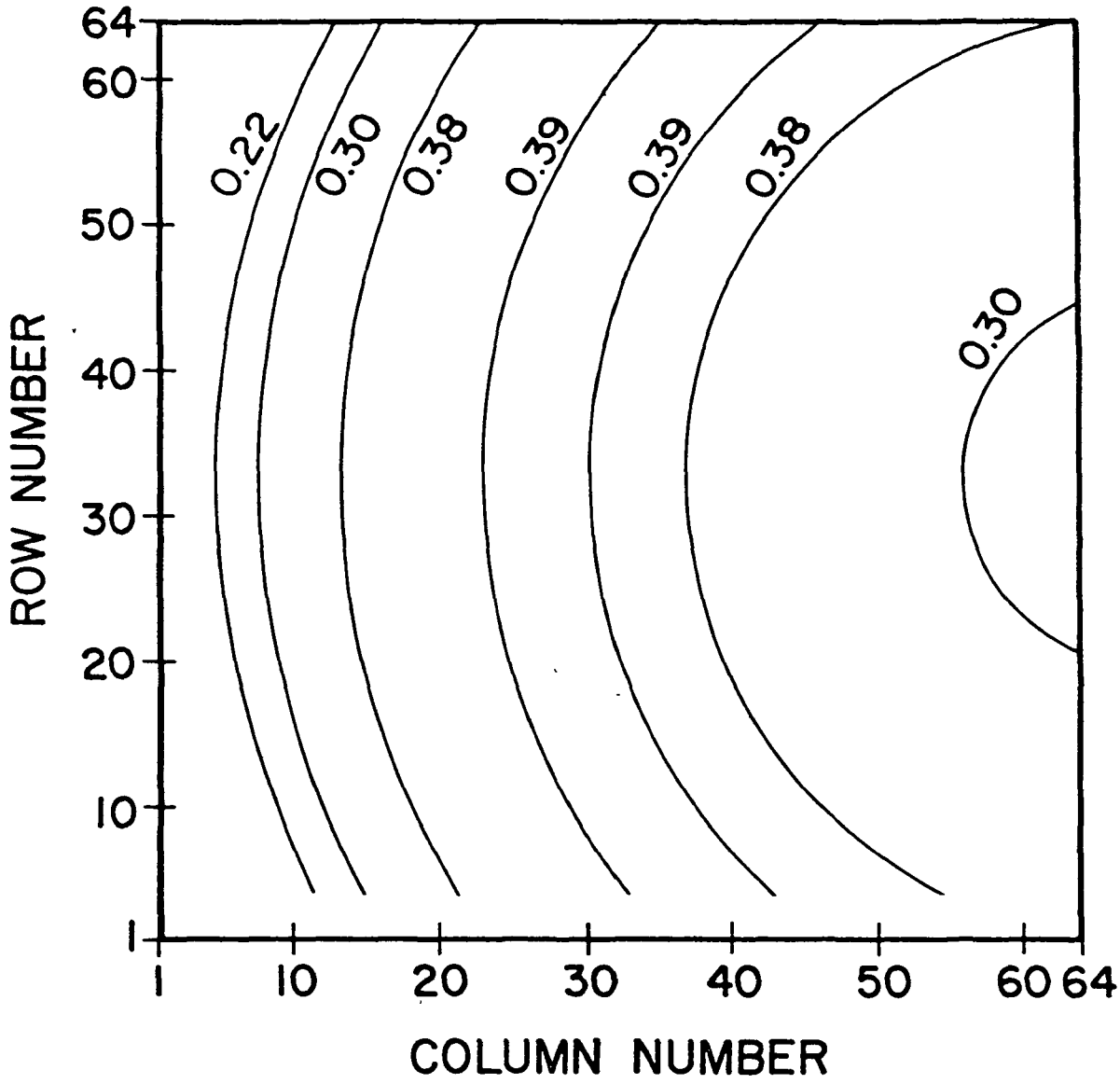
64
60
50
40
30
20
10
1
ROW NUMBER
0.22
0.30
0.38
0.39
0.39
0.38
0.30
1
10
20
30
40
50
60
64
COLUMN NUMBER

Figure 2a

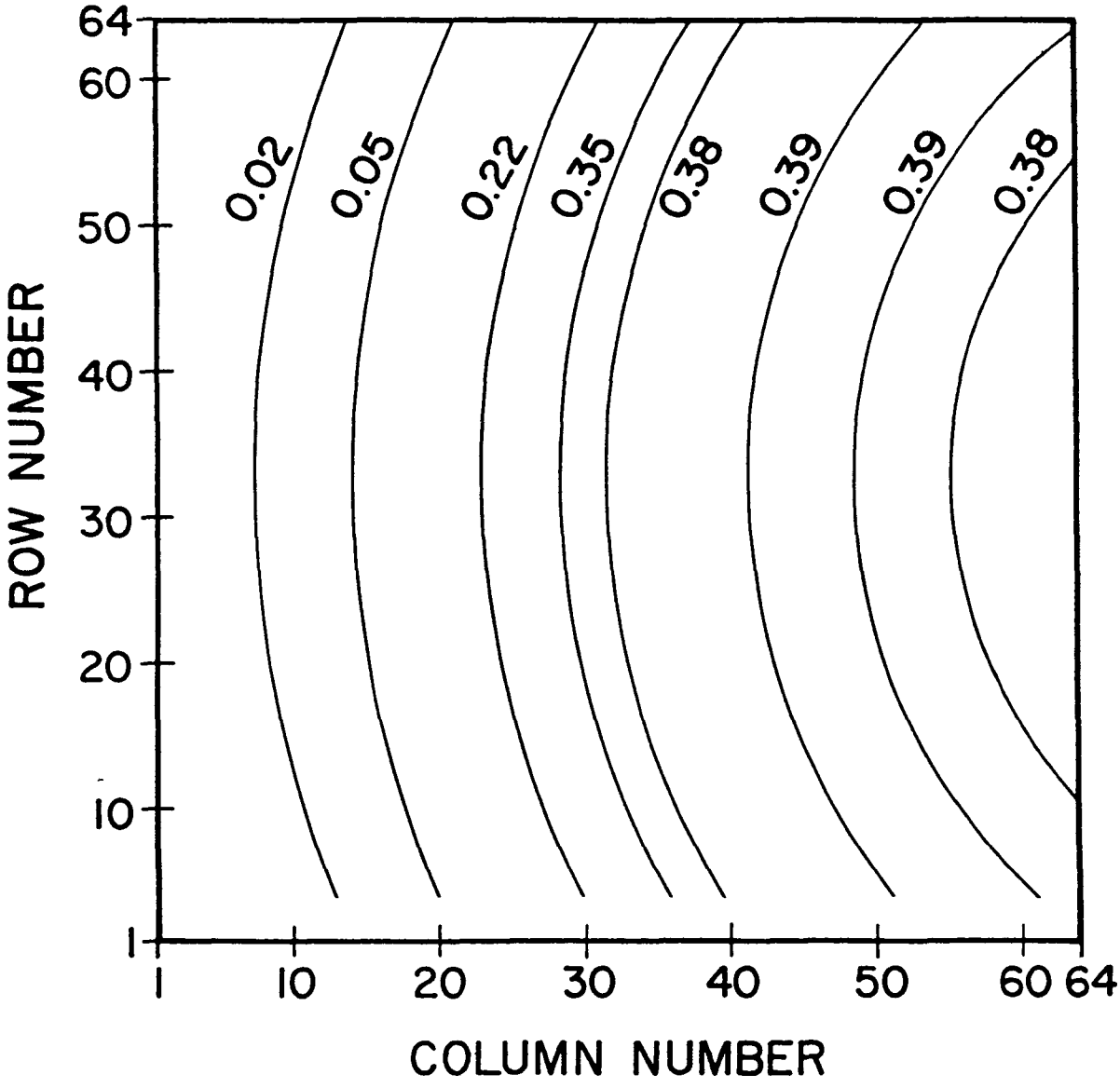
64
60
50
40
30
20
10
1
ROW NUMBER
0.02
0.05
0.22
0.35
0.38
0.39
0.39
0.38
1
10
20
30
40
50
60
64
COLUMN NUMBER

Figure 2b

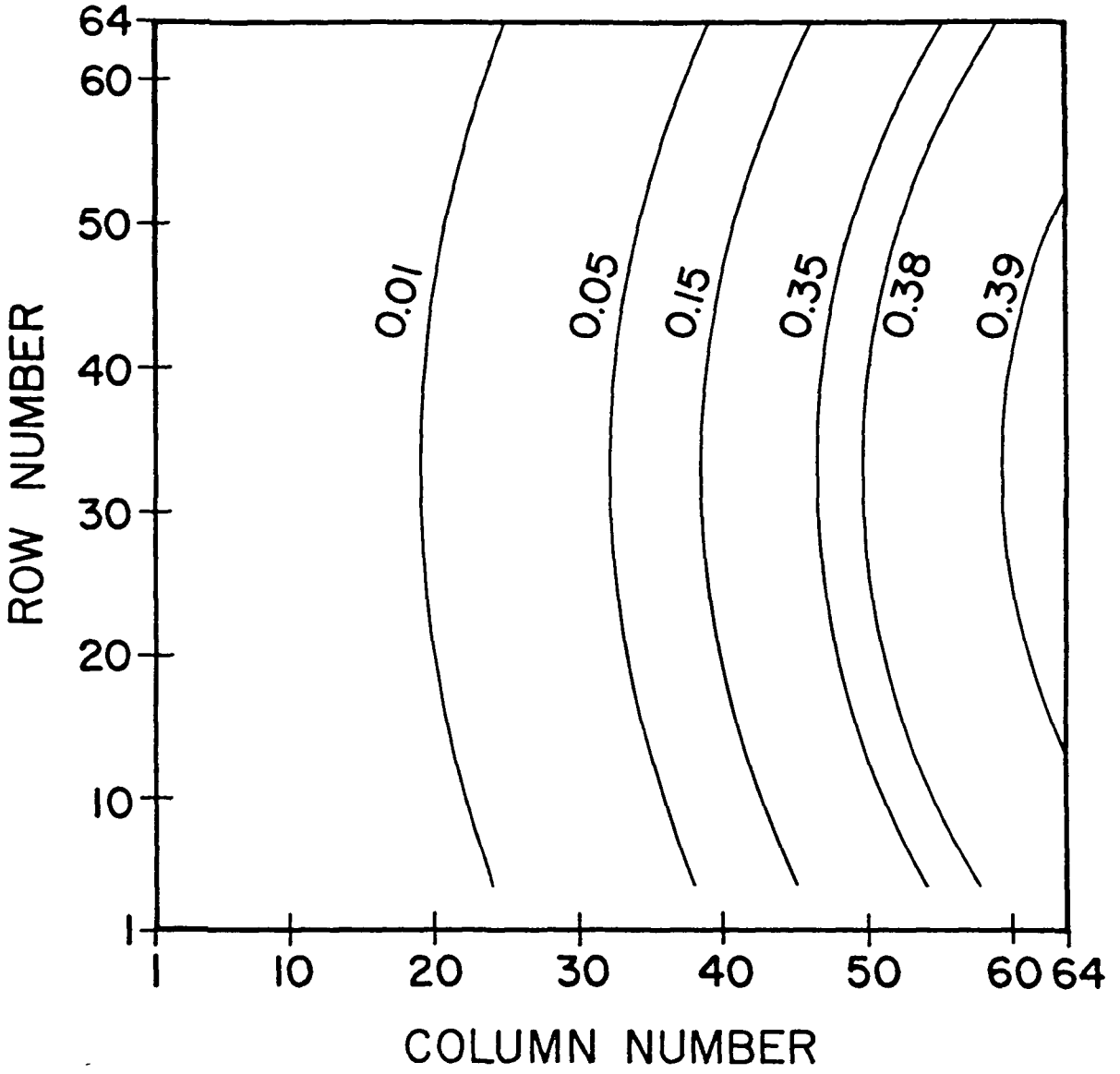
64
60
50
40
30
20
10
1
ROW NUMBER
0.01
0.05
0.15
0.35
0.38
0.39
1
10
20
30
40
50
60
64
COLUMN NUMBER

Figure 2c

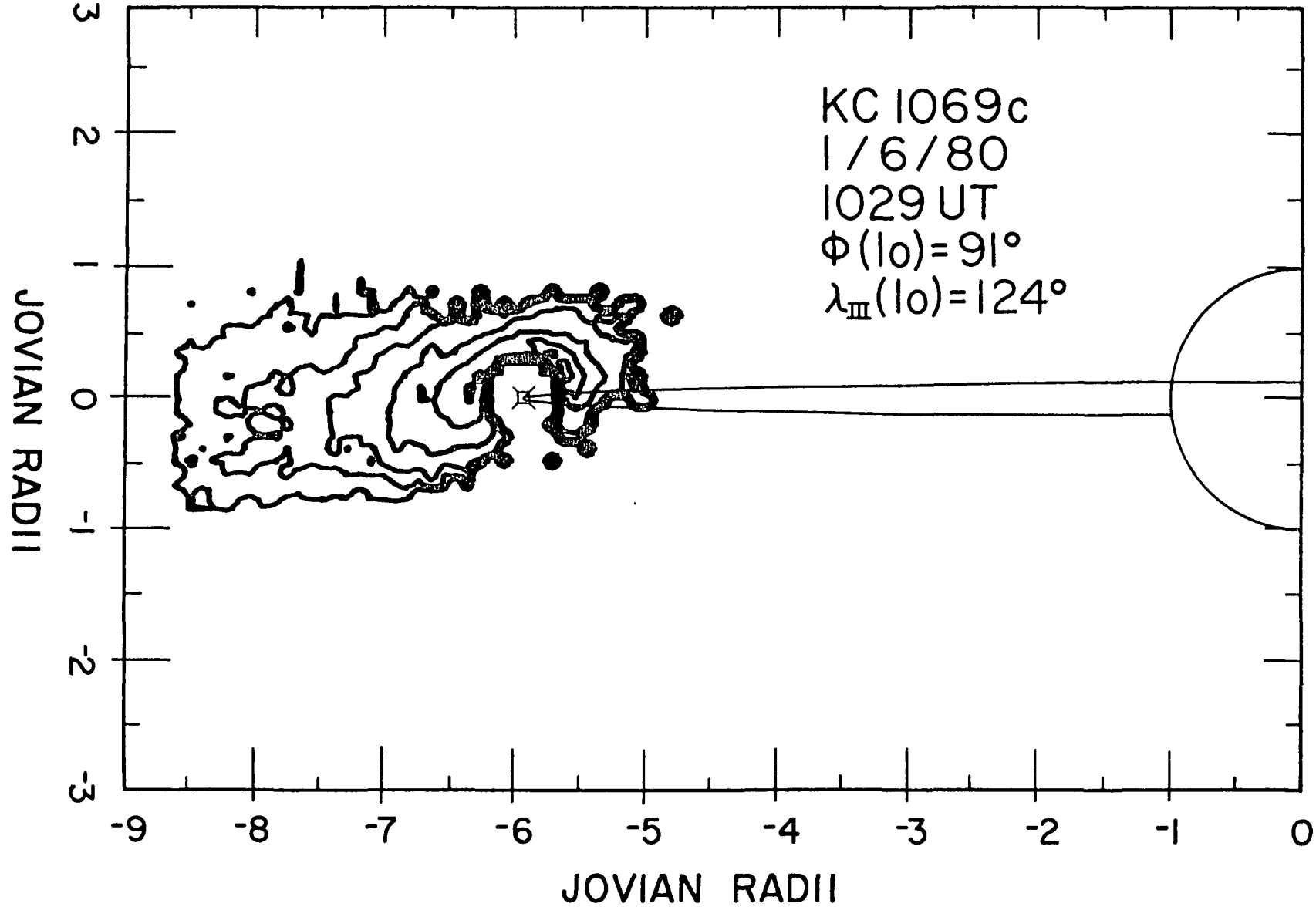
KC 1069c
1/6/80
1029 UT
Φ(Io)=91°
λIII(Io)=124°
JOVIAN RADII
JOVIAN RADII
3
2
1
0
-1
-2
-3
-9
-8
-7
-6
-5
-4
-3
-2
-1
0

Figure 4a

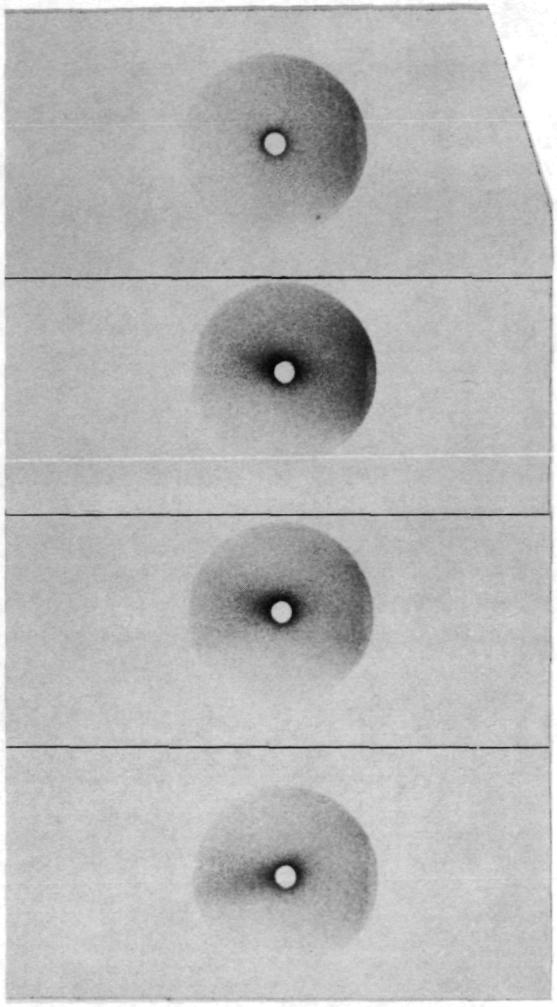

(d) 1073c

(c) 1076a

(b) 1073a

(a) 1069c

Figure 3

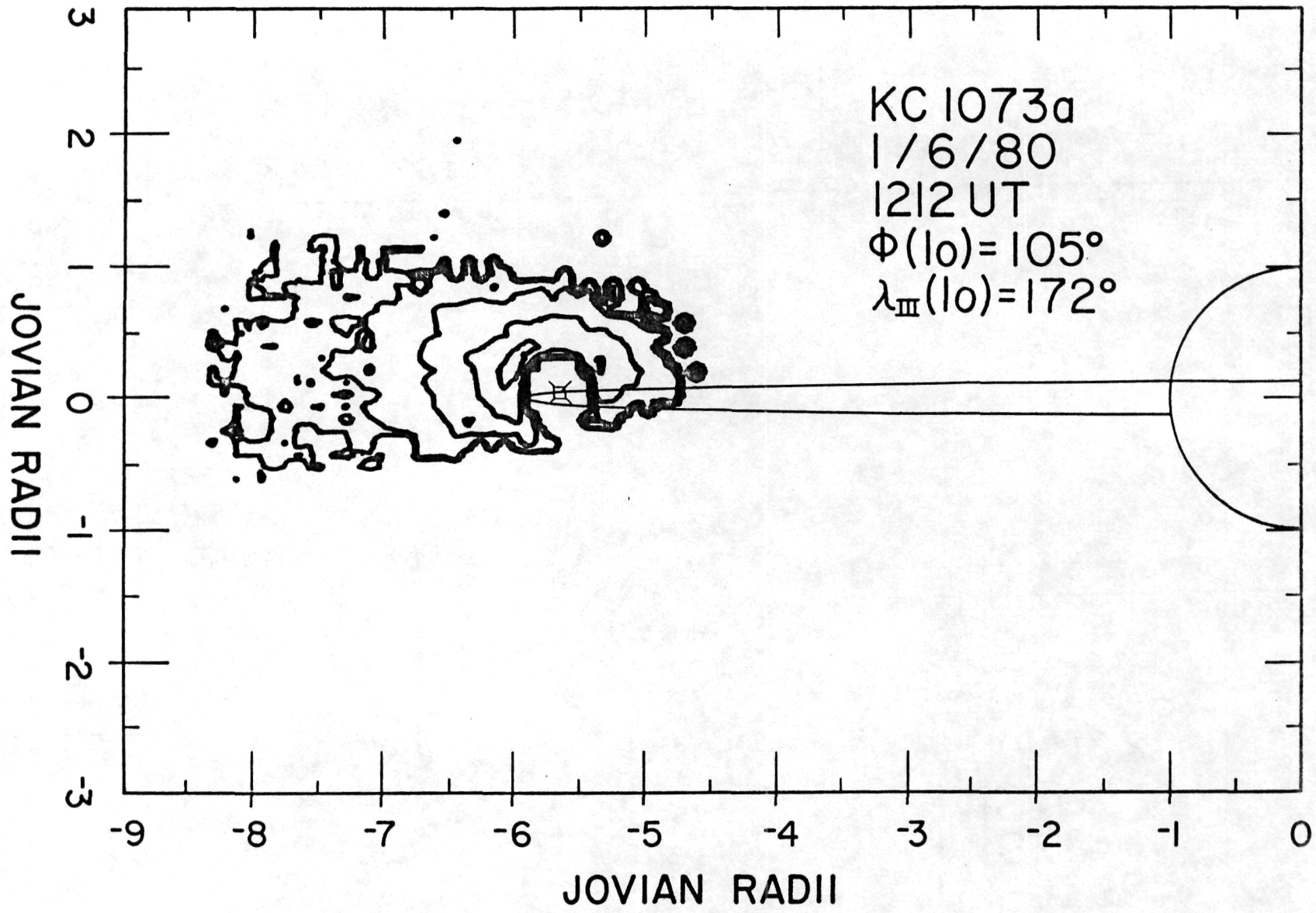
KC 1073a
1/6/80
1212 UT
Φ(Io)=105°
λIII(Io)=172°
JOVIAN RADII
JOVIAN RADII
3
2
1
0
-1
-2
-3
-9
-8
-7
-6
-5
-4
-3
-2
-1
0

Figure 4b

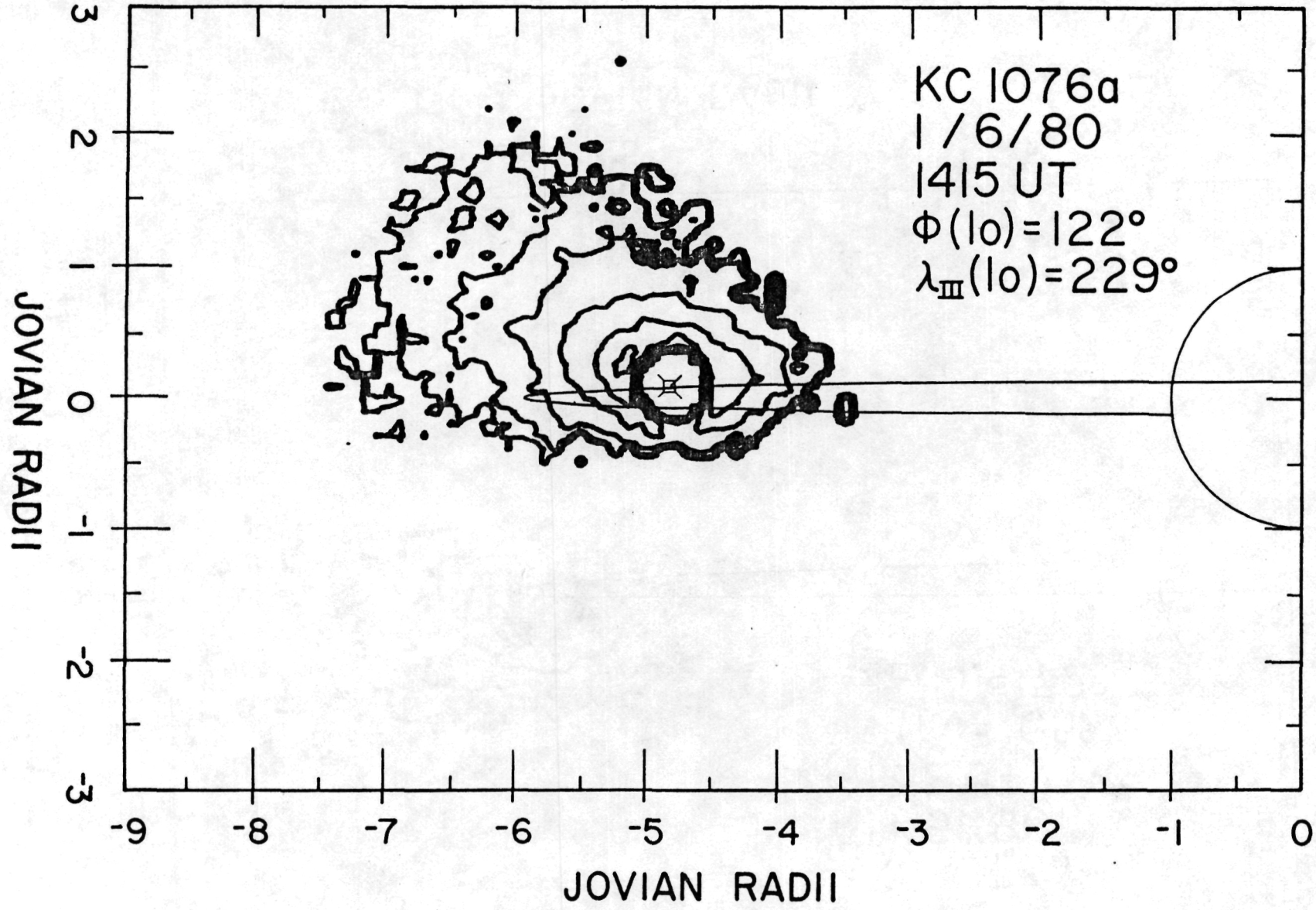
KC 1076a
1/6/80
1415 UT
Φ(Io)=122°
λIII(Io)=229°
JOVIAN RADII
JOVIAN RADII
3
2
1
0
-1
-2
-3
-9
-8
-7
-6
-5
-4
-3
-2
-1
0

Figure 4c

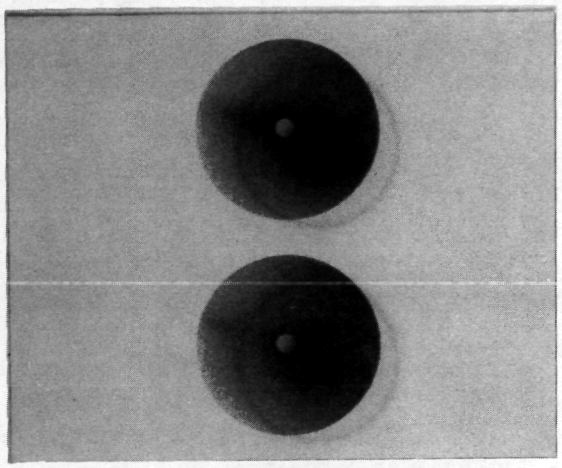

(b) 1845b

(a) 1845a

Figure 5

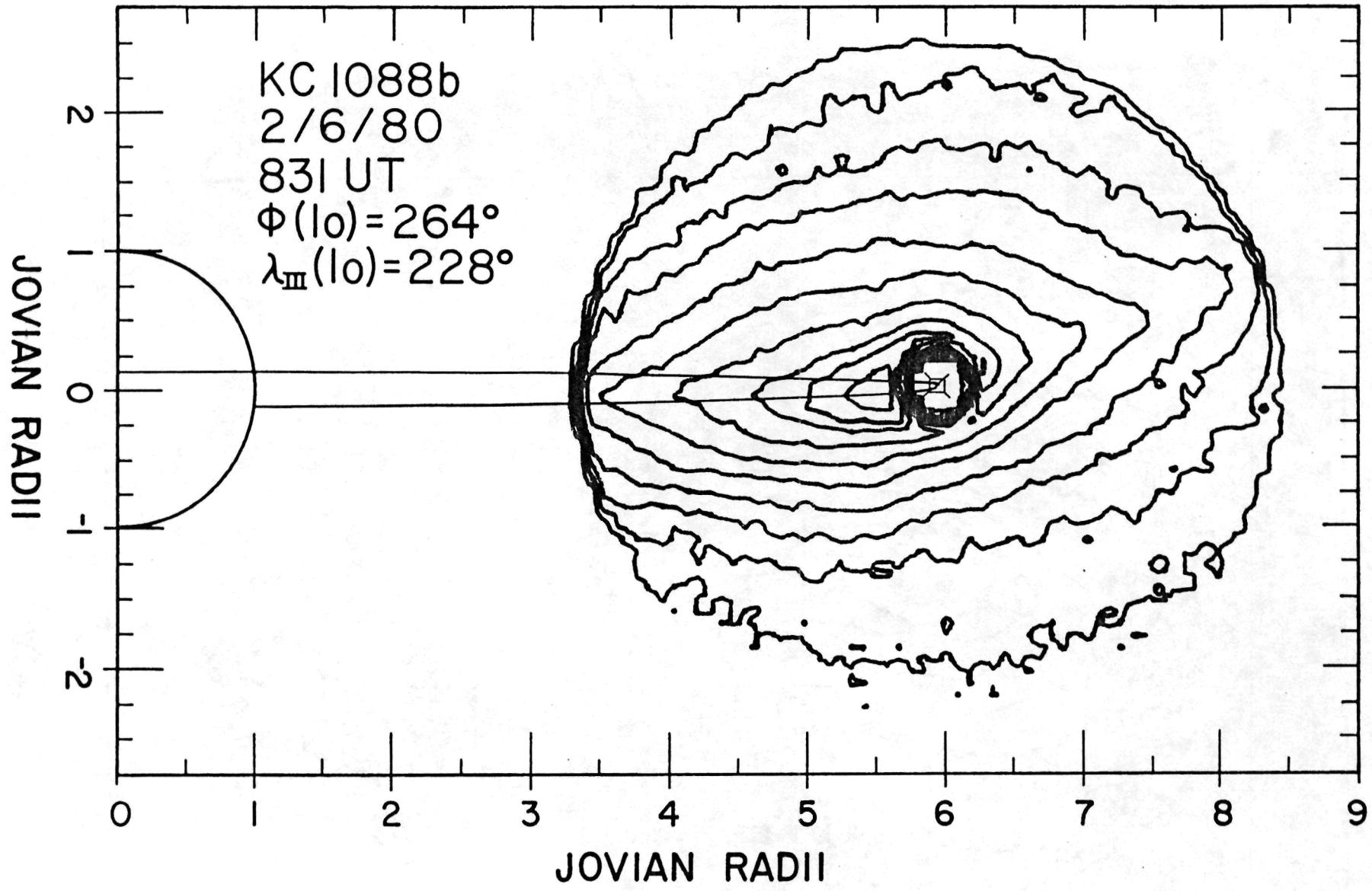
KC 1088b
2/6/80
831 UT
Φ(Io) = 264°
λIII(Io) = 228°
JOVIAN RADII
2
1
0
-1
-2
0
1
2
3
4
5
6
7
8
9
JOVIAN RADII

Figure 6a

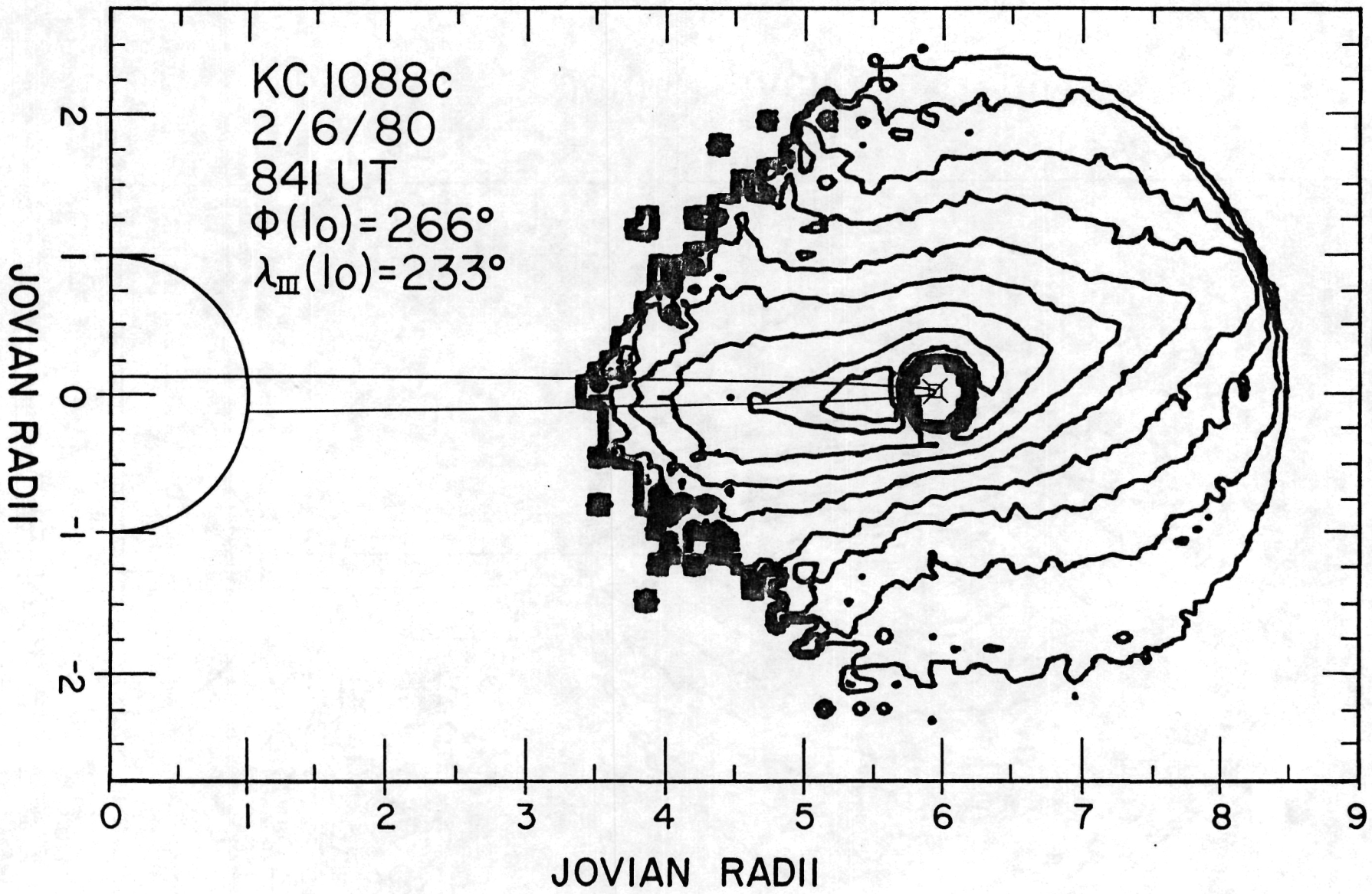
KC 1088c
2/6/80
841 UT
Φ(Io)=266°
λIII(Io)=233°
JOVIAN RADII
2
1
0
-1
-2
0
1
2
3
4
5
6
7
8
9
JOVIAN RADII

Figure 6b

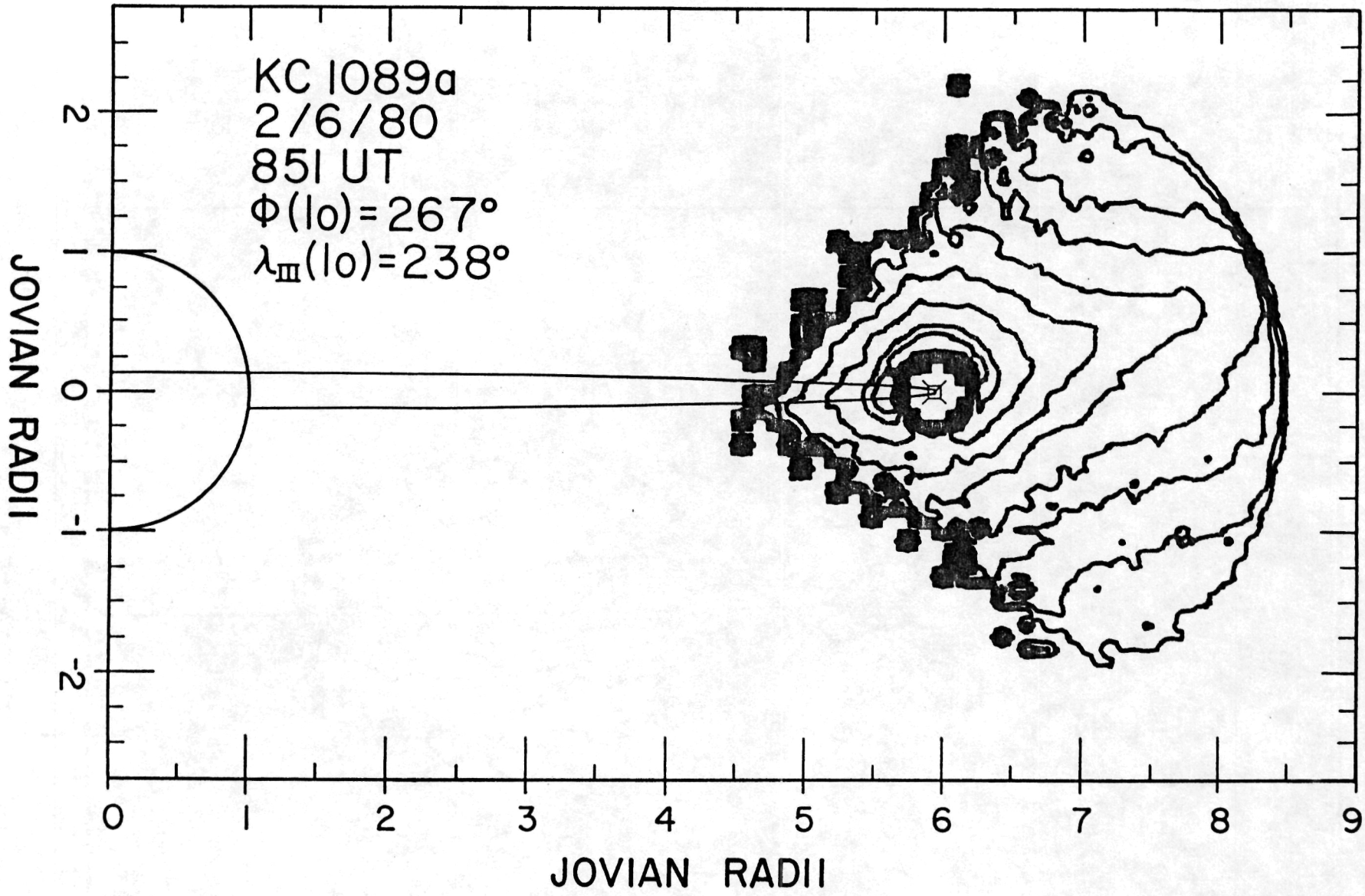
KC 1089a
2/6/80
851 UT
Φ(Io)=267°
λIII(Io)=238°
JOVIAN RADII
2
1
0
-1
-2
0
1
2
3
4
5
6
7
8
9
JOVIAN RADII

Figure 6c

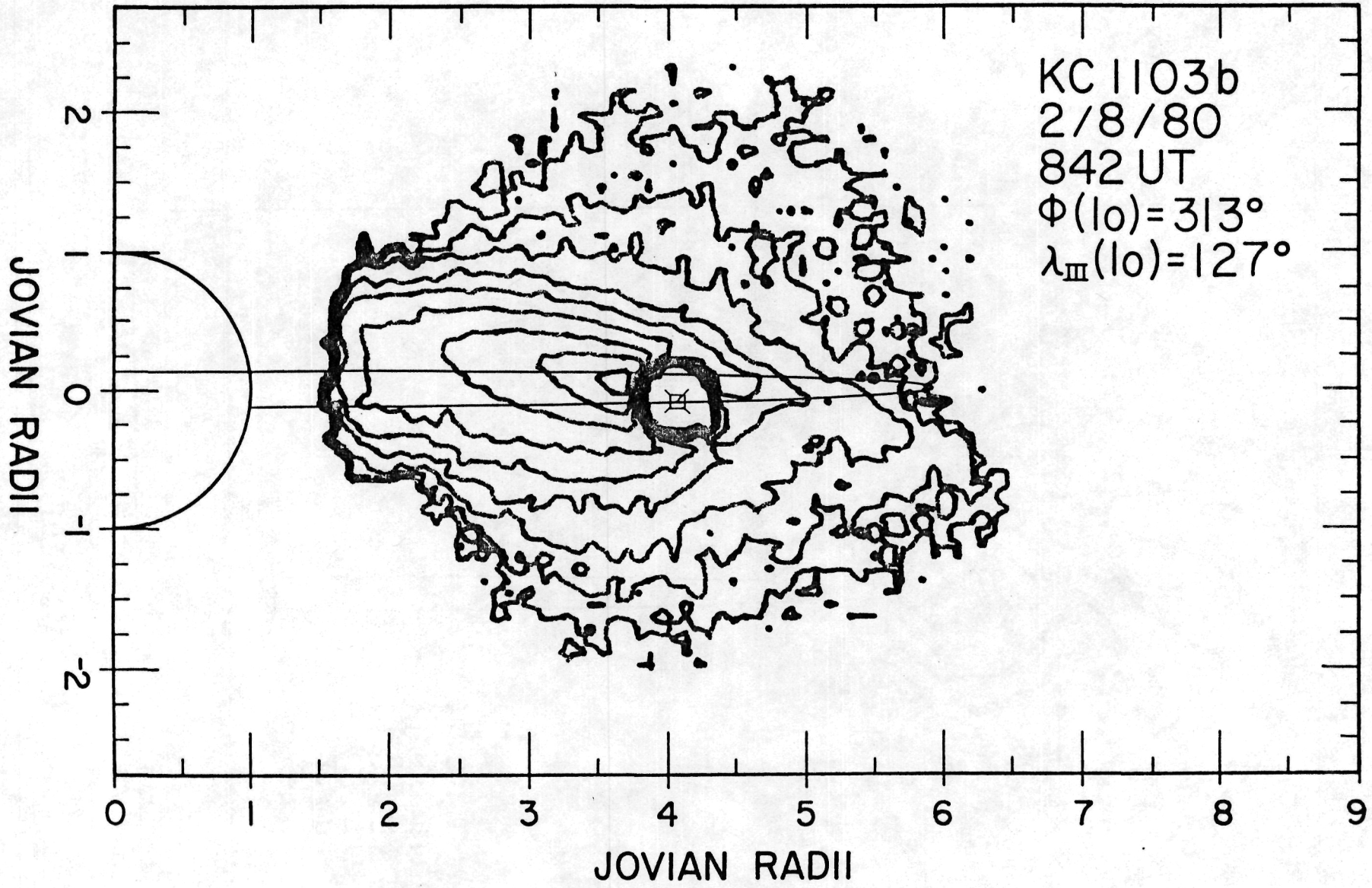
KC 1103b
2/8/80
842 UT
Φ(Io)=313°
λIII(Io)=127°
JOVIAN RADII
JOVIAN RADII
2
1
0
-1
-2
0
1
2
3
4
5
6
7
8
9

Figure 7d

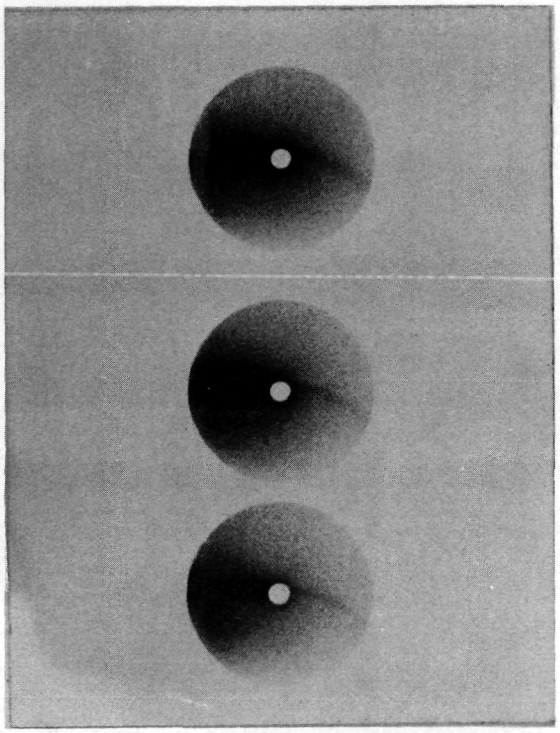

(c) 1103c

(b) 1103b

(a) 1103a

Figure 7a-c

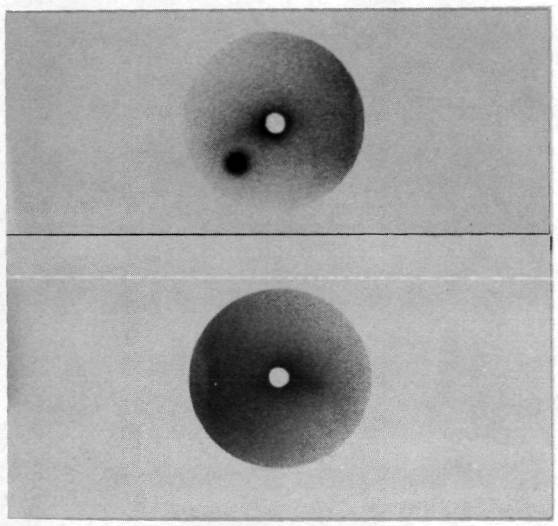

(b) 1456a

(a) 1838c

Figure 8

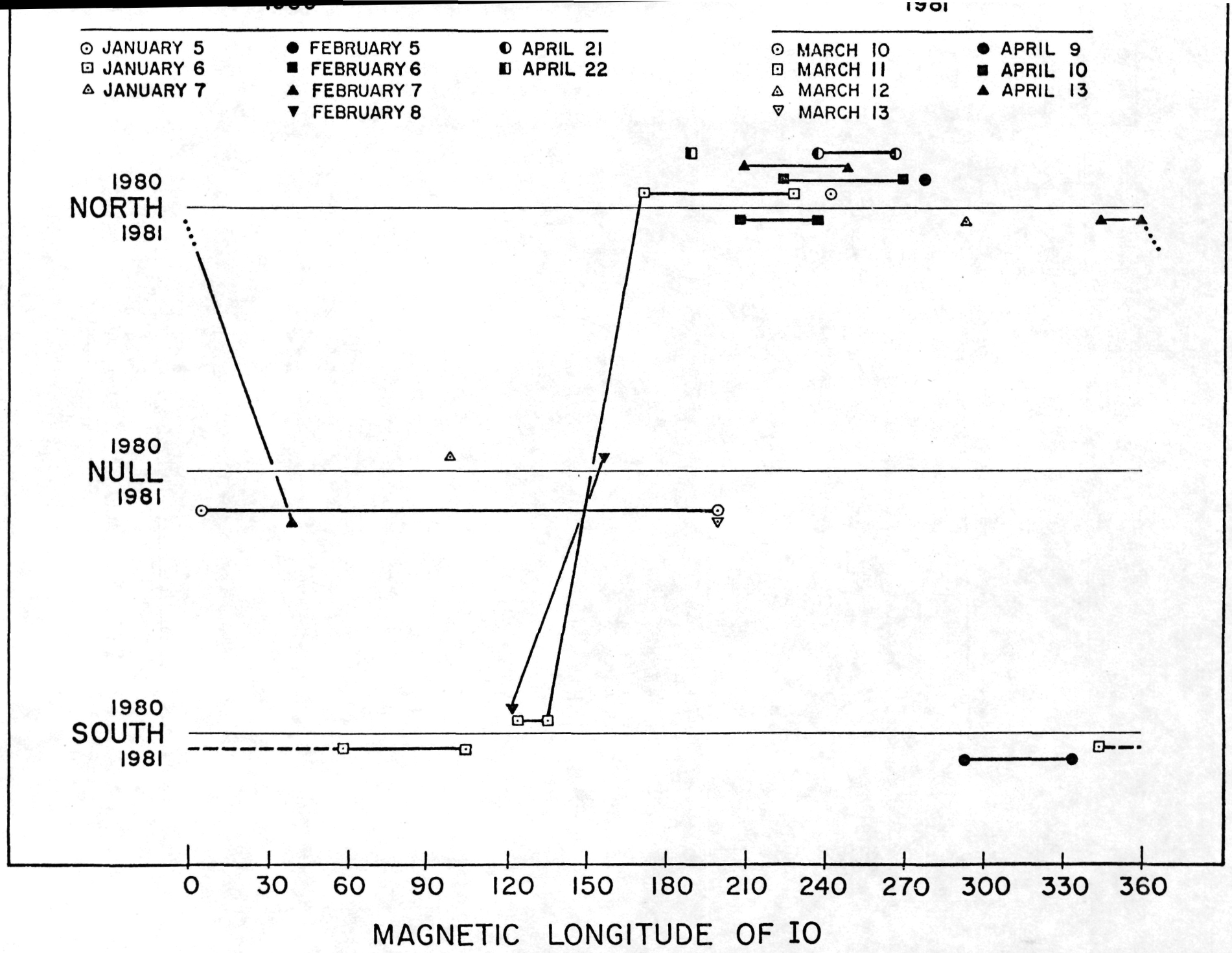
1981
JANUARY 5
JANUARY 6
JANUARY 7
FEBRUARY 5
FEBRUARY 6
FEBRUARY 7
FEBRUARY 8
APRIL 21
APRIL 22
MARCH 10
MARCH 11
MARCH 12
MARCH 13
APRIL 9
APRIL 10
APRIL 13
1980
NORTH
1981
1980
NULL
1981
1980
SOUTH
1981
0
30
60
90
120
150
180
210
240
270
300
330
360
MAGNETIC LONGITUDE OF IO

Figure 9

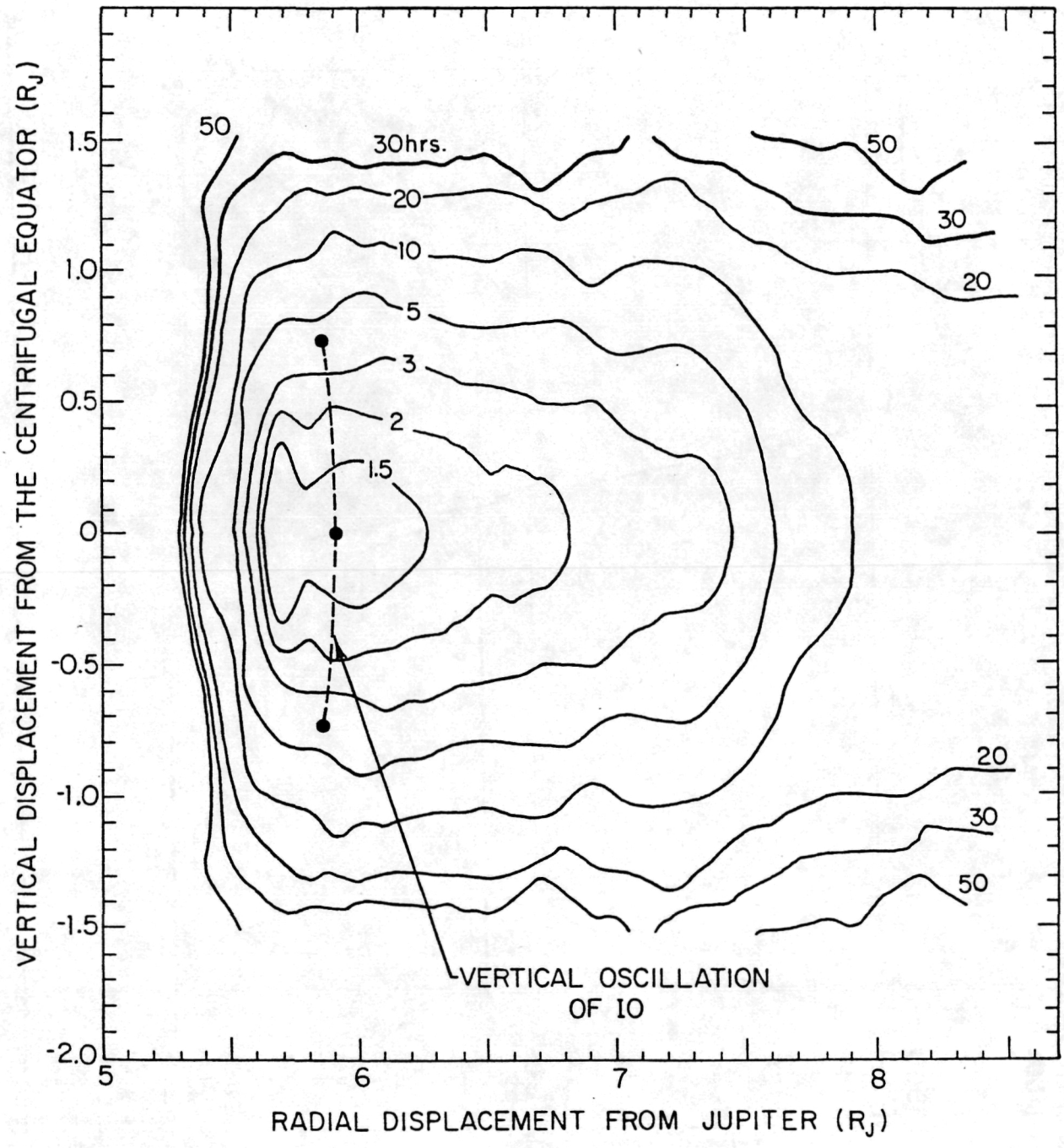
VERTICAL DISPLACEMENT FROM THE CENTRIFUGAL EQUATOR (R_J)
RADIAL DISPLACEMENT FROM JUPITER (R_J)
1.5
1.0
0.5
0
-0.5
-1.0
-1.5
-2.0
5
6
7
8
50
30hrs.
20
10
5
3
2
1.5
50
30
20
20
30
50
VERTICAL OSCILLATION
OF IO

Figure 10

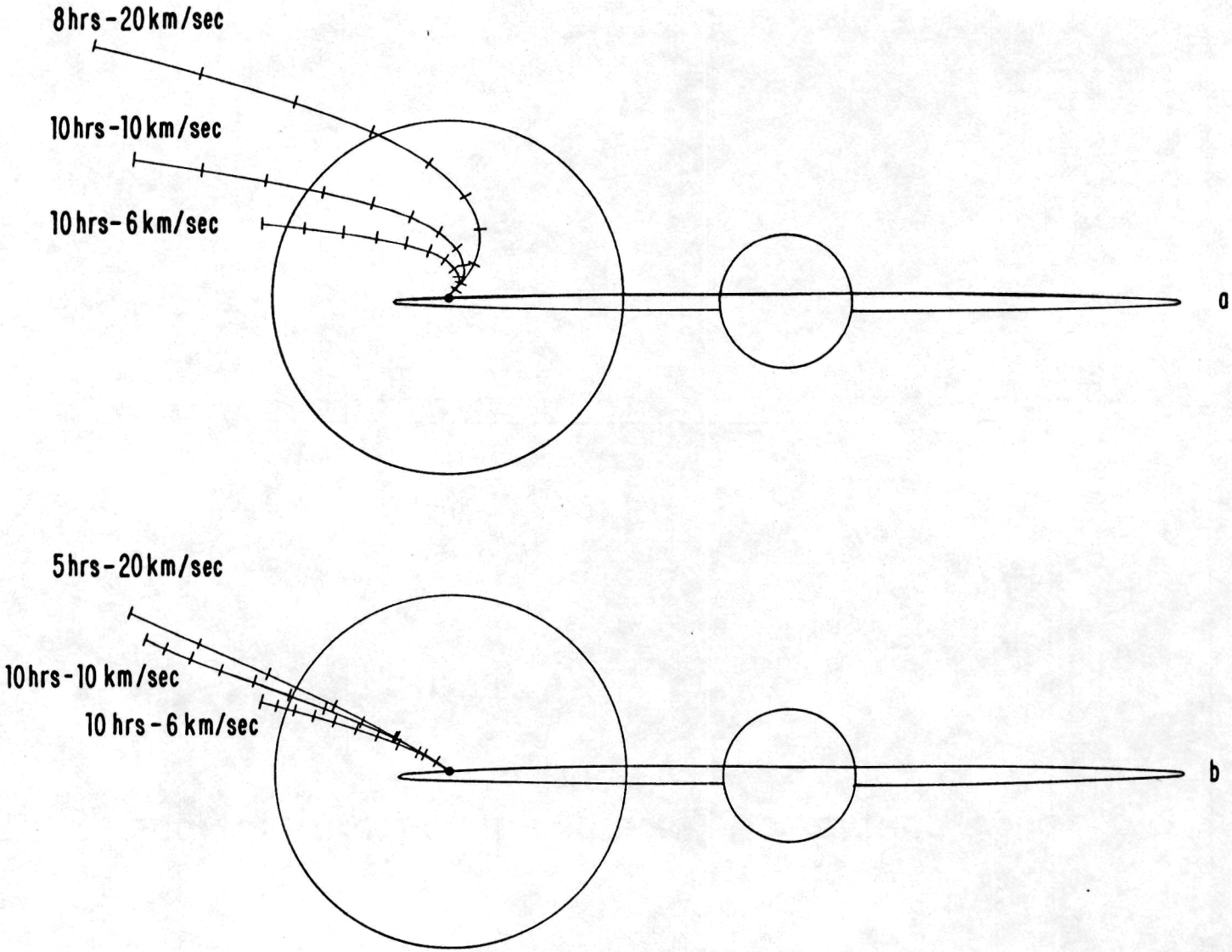
8hrs - 20km/sec
10hrs - 10km/sec
10hrs - 6km/sec
a
5hrs - 20km/sec
10hrs - 10 km/sec
10 hrs - 6 km/sec
b

Figure 11

Sodium Directional Features: Correlation Study

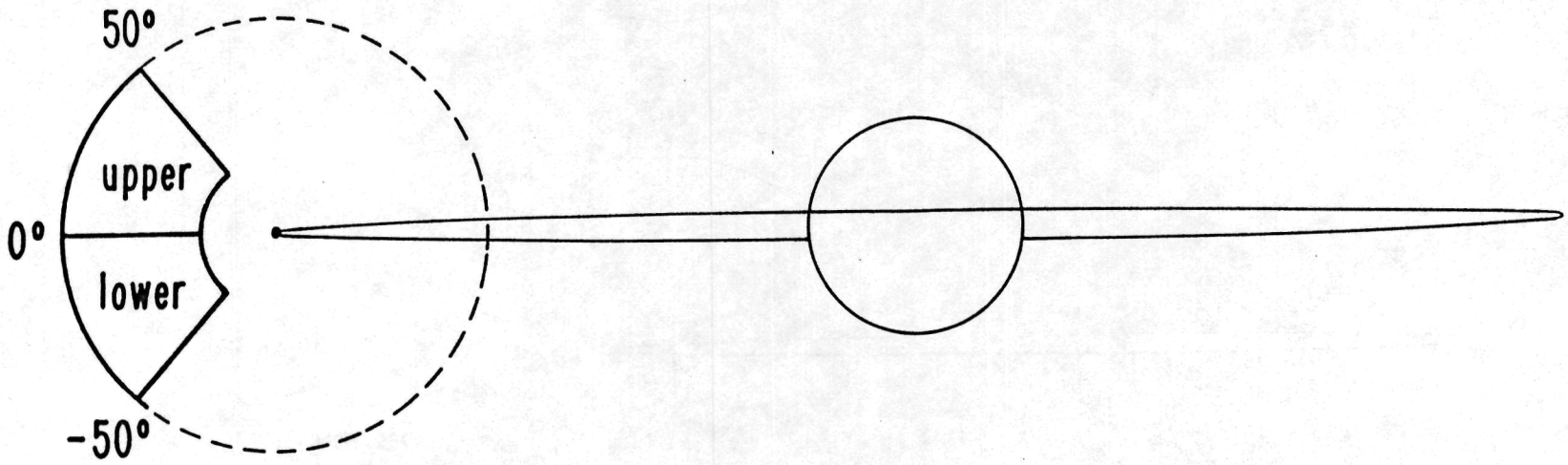

Figure 12

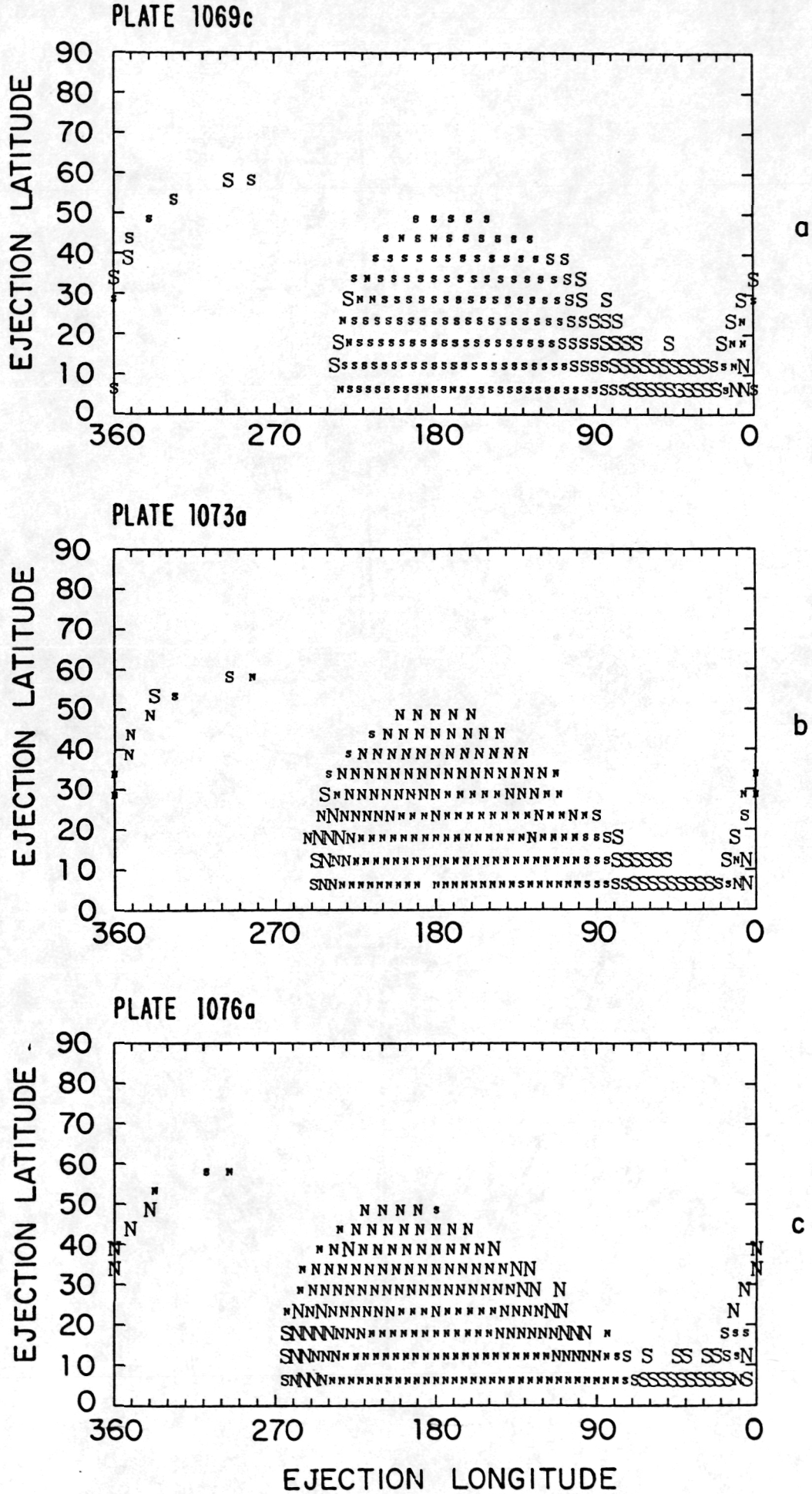
PLATE 1069c
EJECTION LATITUDE
90
80
70
60
50
40
30
20
10
0
360
270
180
90
0
a
PLATE 1073a
EJECTION LATITUDE
b
PLATE 1076a
EJECTION LATITUDE
c
EJECTION LONGITUDE

Figure 13

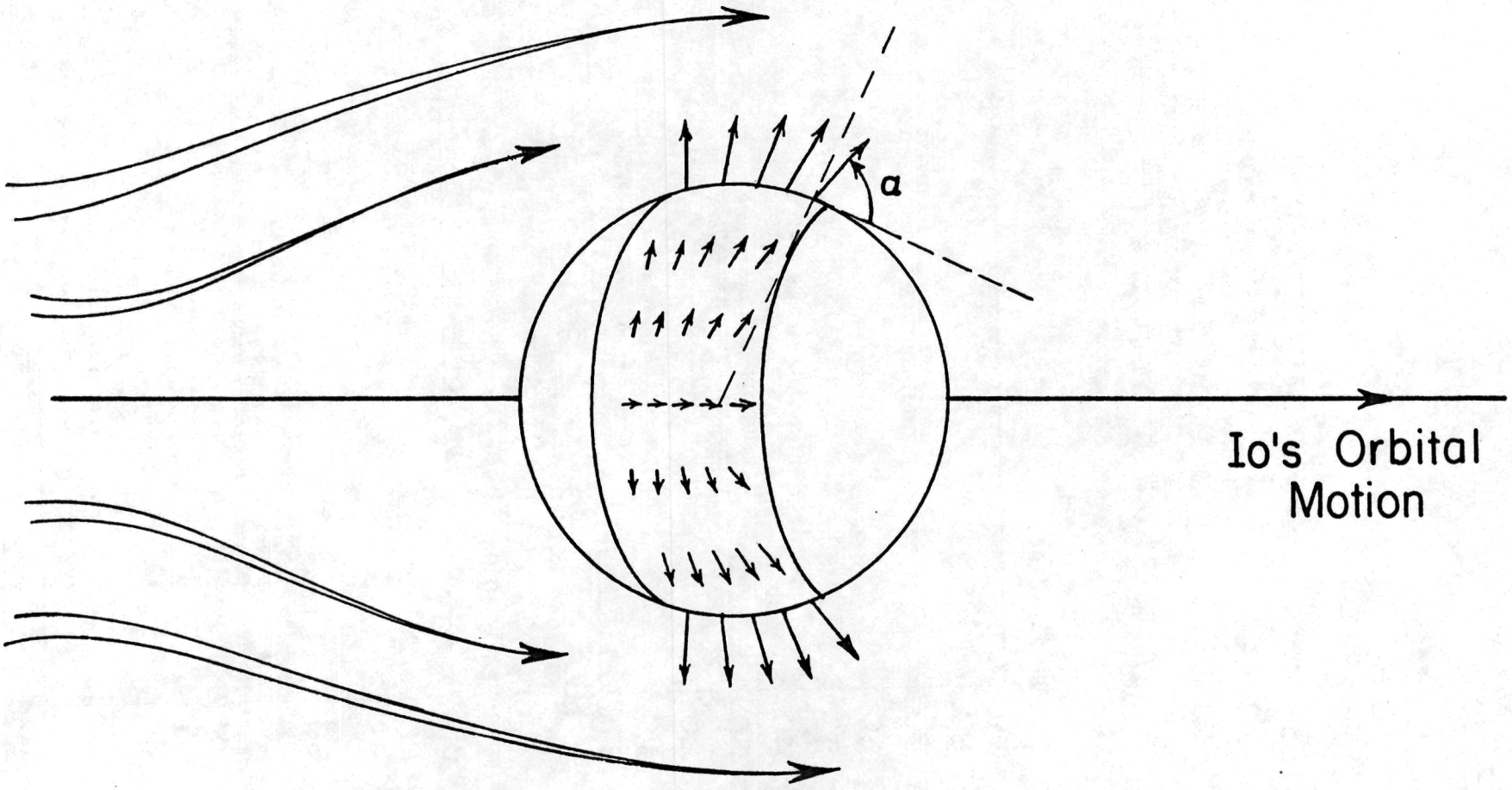

Figure 14

PLATE 1069c

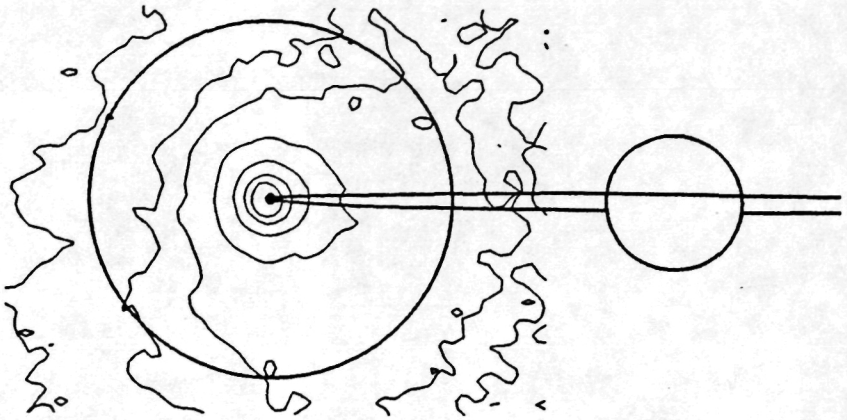

PLATE 1073a

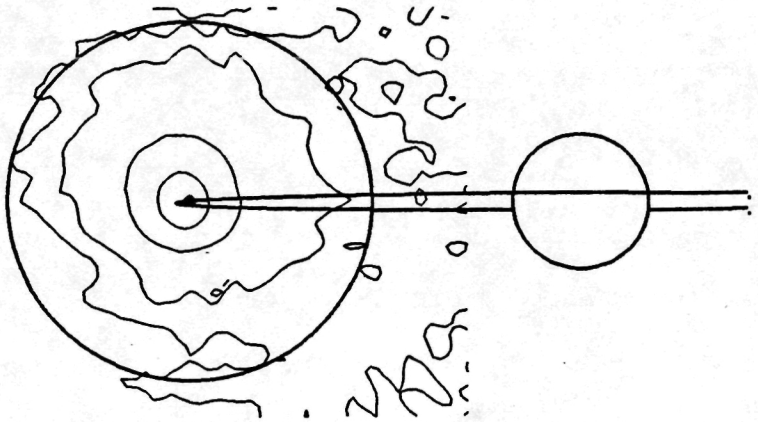

PLATE 1076a

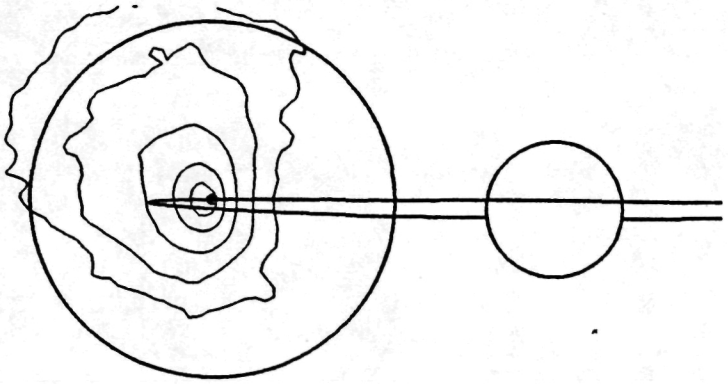

Figure 15

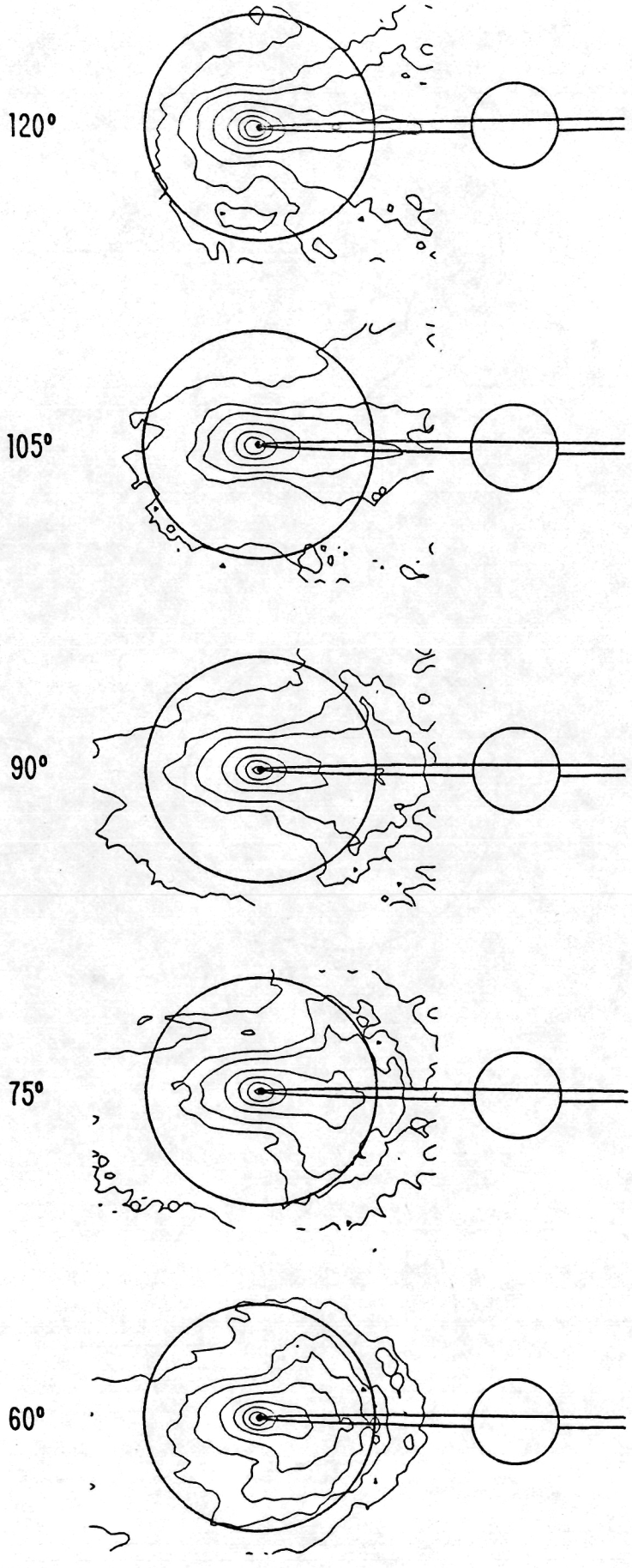

Figure 16

PLATE 1069c

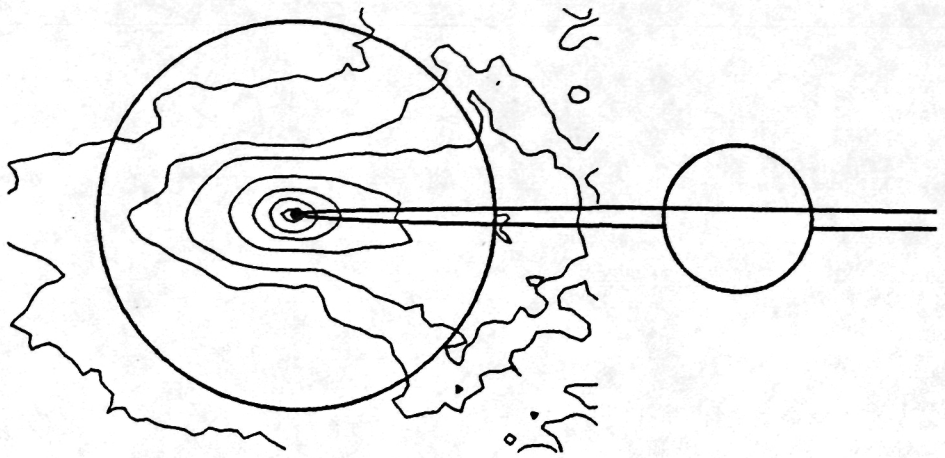

PLATE 1073a

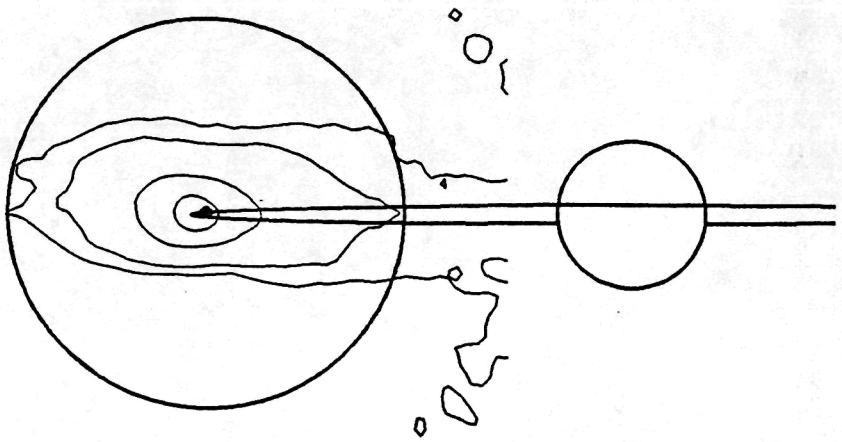

PLATE 1076a

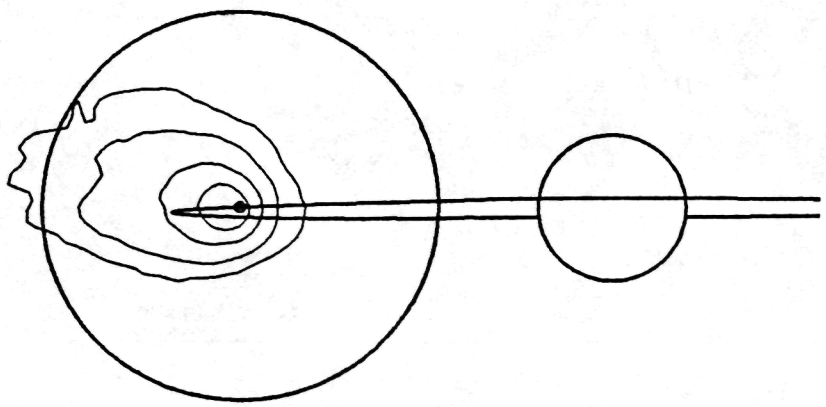

Figure 17

PLATE 1069c

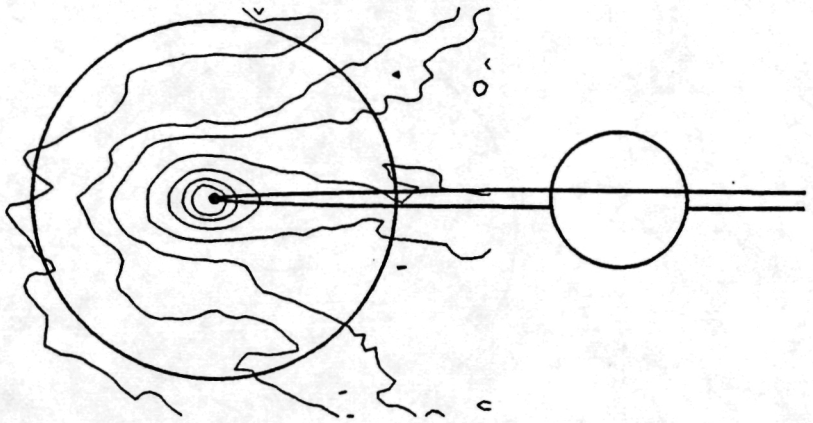

PLATE 1073a

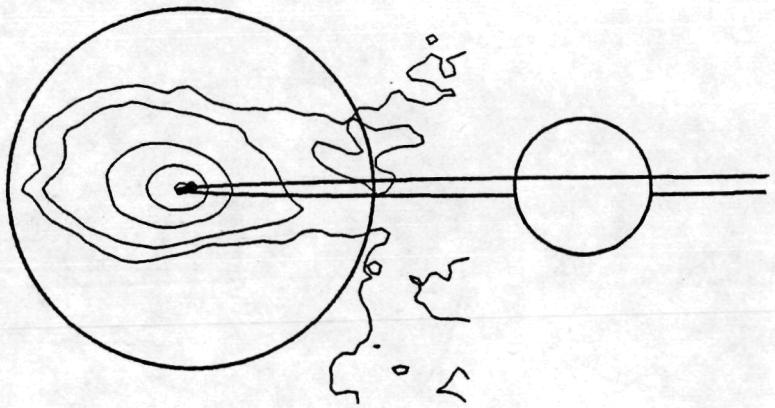

PLATE 1076a

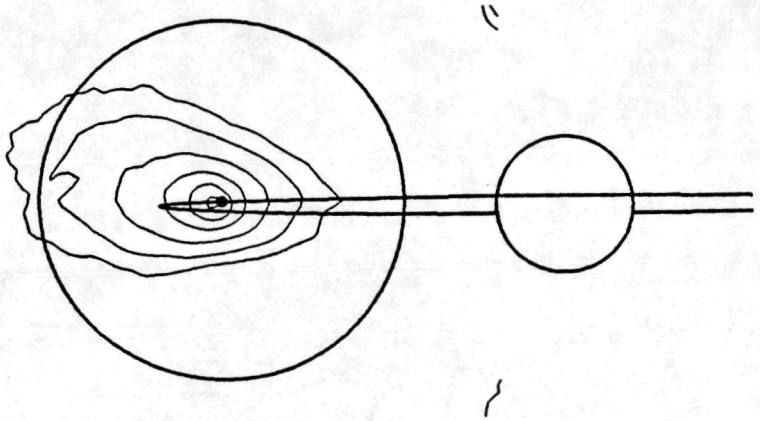

Figure 18

PLATE 1069c

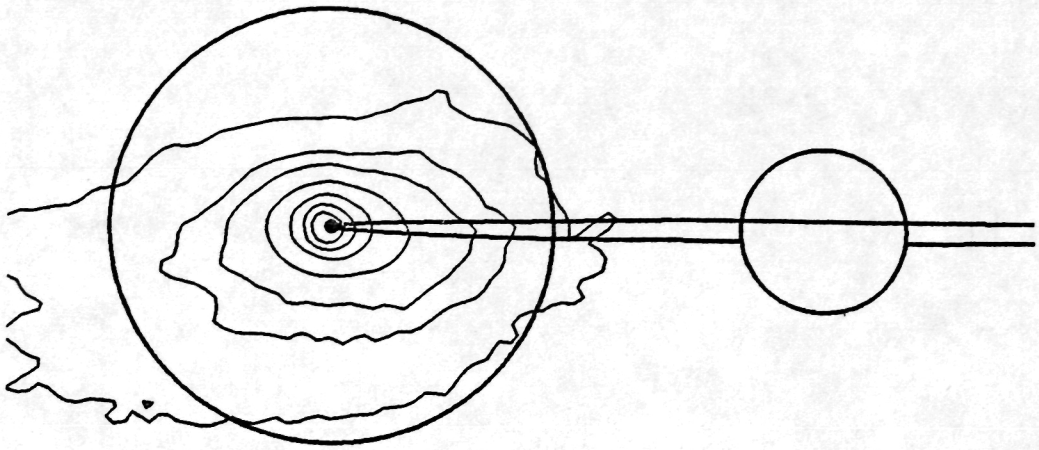

PLATE 1073a

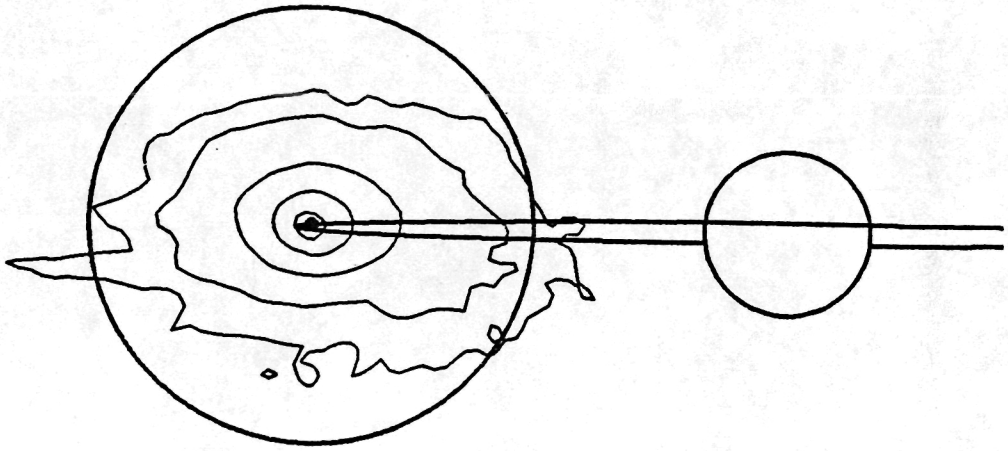

PLATE 1076a

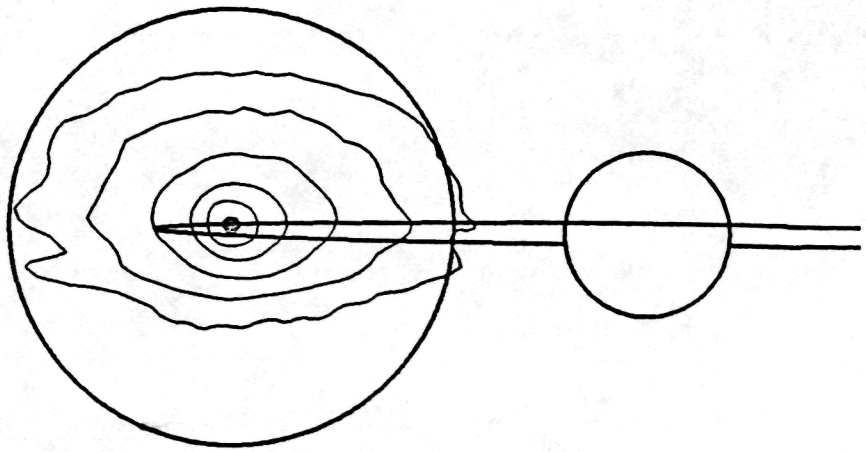

Figure 19

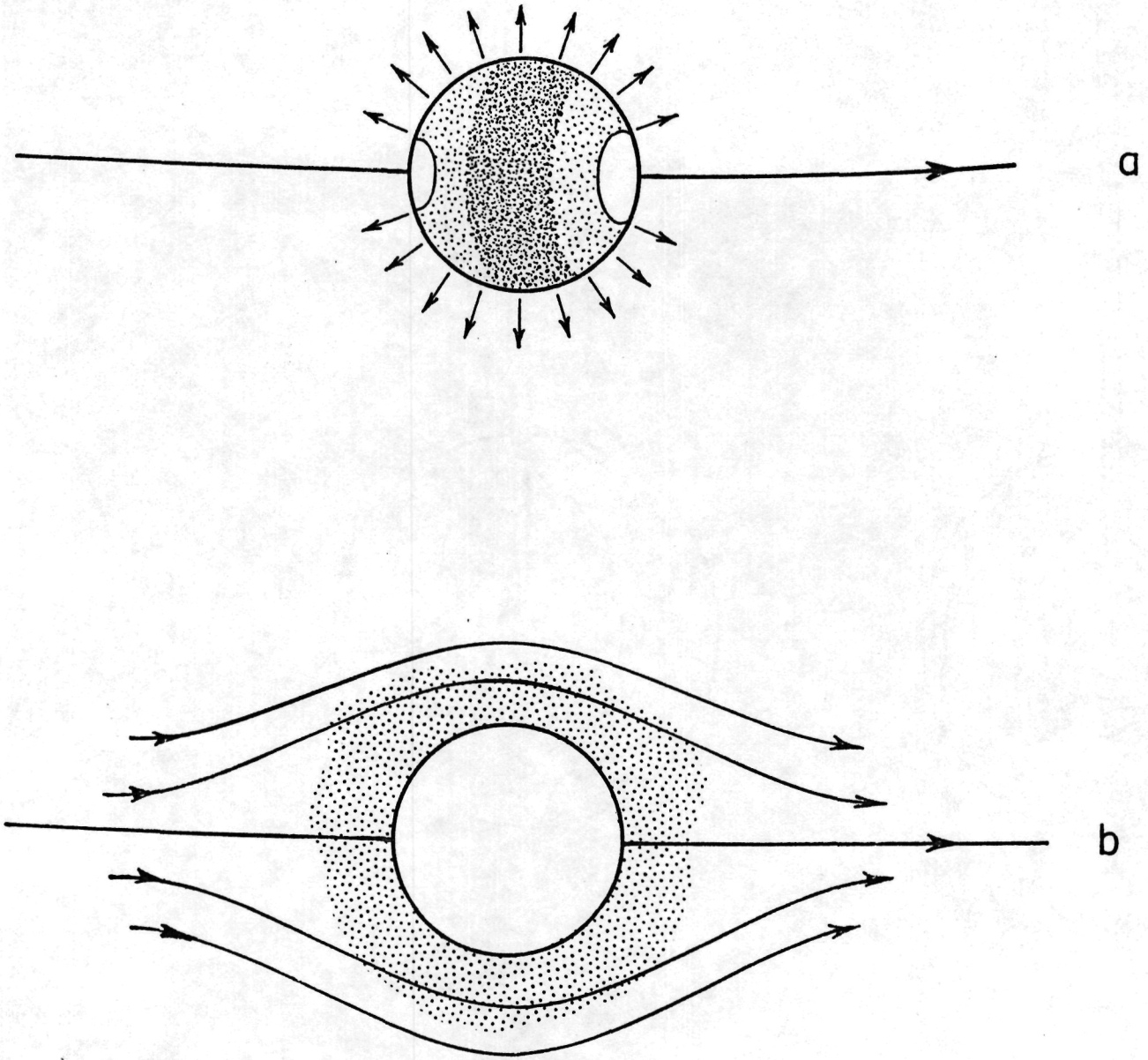

Figure 20